MATHEMATICAL MODELING OF MALARIA TRANSMISSION AND TREATMENT: A CASE OF CONFLICT ZONES

NGUU ALEX NG'ATIA

A Thesis Submitted to the Graduate School in Partial Fulfilment of the Requirements for the Award of the Degree of Master of Science in Applied Mathematics of Tharaka University

THARAKA UNIVERSITY

NOVEMBER 2025

DECLARATION AND RECOMMENDATION

Declaration

This Thesis is my original work and has not been presented for an award of diploma or conferment of degree in any other University.

Signature:..... Date: 19/11/2025

Nguu Alex Ngátia
SMT12/10061/23

Recommendation

This Thesis has been examined, passed and submitted with our approval as university supervisors.

Signature:..... Date: 19/11/2025

Dr. Jomba Jason, PhD.
Tharaka University.

Signature:..... Date: 19/11/2025

Mr. Ngari Charles
Kirinyaga University.

COPYRIGHT @ 2025

All rights reserved. No part of this thesis may be reproduced or transmitted in any form or by any electronic or mechanical means including photocopying, recording or any information retrieval system without permission in writing from the author or Tharaka University.

DEDICATION

This study is dedicated to my parent Lydia, my brother Felix, my spouse Winfred and my child Queensfine for their unconditional love, patience, and steadfast support throughout this journey.

ACKNOWLEDGMENTS

I express deep appreciation to the Almighty God for His guidance. Thank you to supervisors, Mr. Charles Ngari and Dr. Jason Jomba for their essential support in completing this research. Appreciation is also extended to the Department of Physical Sciences at Tharaka University for the resources provided, and to the faculty for their valuable feedback, and to my colleagues for their support and support. I am especially indebted to my family, Winfred Mwende in conjunction with Queensfine Kawira in recognition of financial assistance as well as peace of mind during the research writing.

ABSTRACT

Malaria continues to be among the most pressing public health challenges globally, disproportionately affecting vulnerable populations in tropical and subtropical regions. The infection is spread through the bites of female Anopheles mosquitoes carrying the parasite, with high-risk groups including people with compromised immune systems and travelers to endemic areas. Despite extensive control efforts and the formulation of mathematical models that integrate essential biological and pharmacological components such as human immunity level, vector behavior treatment coverage and drug resistance, significant gaps persisted in understanding malaria transmission and treatment dynamics, particularly in conflict-affected zones. The study develops a mathematical model for malaria transmission and treatment in conflict zones capturing interventions such as full treatment and partial treatment. The model utilizes a system of ordinary differential equations (ODEs) to describe the progression describing malaria transmission and treatment over time, capturing transitions across different human and mosquito compartments. The positivity of solutions was established to ensure biological feasibility. The existence of a Disease-Free Equilibrium (DFE) was determined and found that no infection exist in human population. Stability analysis was conducted to assess the conditions under which malaria can be eliminated, while sensitivity analysis identified key parameters that significantly influenced transmission and treatment outcomes. Numerical simulations were performed using Mathematica and python software to validate the analytical results and examine the effects of control measures under varying conditions. The findings provided insights into the effectiveness of treatment strategies and interventions aimed at reducing malaria transmission and mortality in conflict zones. The study also offered evidence-based recommendations applicable to similar health-constrained environments.

TABLE OF CONTENTS

LIST OF FIGURES

SYMBOLS AND INDEX OF NOTATIONS

$\wedge$	Recruitment of susceptible mosquitoes
e	Death rate of full treatment humans
$E(t)$	Exposed humans at time t
$I_C(t)$	Number of infected humans in conflict zones
$I_f(t)$	Infected humans in other zones
$I_V(t)$	Infectious mosquitoes
N	Total population
$S_H(t)$	Number of susceptible humans at time t
$S_V(t)$	Number of susceptible mosquitoes
τ	Death rates of infectious mosquitoes
$T_n(t)$	Treatment of humans being compromised or under dose
$T_p(t)$	Full treatment of humans
υ	Rate of infection of mosquitoes from other zones
X	Recovery rate of full treatment humans
Z	Rate of infected mosquito bites to susceptible humans
α	Rate of infection of humans
γ	Recovery rate of humans in other zones
ϵ	Death rates of compromised humans
Θ	Death rates of infected humans in conflict zones
λ	Infectious rate of humans in conflict zones
μ	Natural death rates of humans

π	Recruitment of susceptible humans
ρ	Rate of recovered exposed humans
ψ	Rate of infection of mosquitoes
ω	Treatment rate for infected humans undergoing full treatment
Φ	Rate of infection of mosquitoes from other zones

ABBREVIATION AND ACRONYMS

ABMs	Agent-based models
ACTs	Artemisinin-based combinations
ARDs	Acute respiratory distress syndrome
CDC	Center for Disease Control and Prevention
DFE	Disease-Free Equilibrium
IRS	Indoor residual spraying
ITNs	Insecticide-treated bed nets
LLINs	Long-lasting insecticidal nets
MATLAB	Matrix laboratory
ODEs	Ordinary differential equations
PK-PD	Pharmacokinetic-pharmacodynamics
RBCs	Red blood cells
R_0	Basic reproduction number
RTDs	Rapid diagnostic tests
SEIR	Susceptible–Exposed–Infected–Recovered
SI	Susceptible–Infected
SIR	Susceptible–Infected–Recovered
WHO	World Health Organization

CHAPTER ONE

INTRODUCTION

1.1 Background Information

According to WHO (2023), malaria is a life-threatening disease caused by parasites of the genus *Plasmodium*, transmitted to humans through the bites of infected female *Anopheles* mosquitoes. WHO (2022) further reported that malaria can also be transmitted congenitally, from an infected mother to her unborn child, or through blood transfusion. Despite being both preventable and curable, WHO (2023) highlights that malaria continues to pose a significant public health challenge, particularly in tropical and subtropical regions. There are five species of *Plasmodium* responsible for malaria in humans: *Plasmodium falciparum* (the most lethal), *Plasmodium vivax*, *Plasmodium ovale*, *Plasmodium malariae*, and *Plasmodium knowlesi* (less common but capable of infecting humans).

According to WHO (2023), in 2022 there were an estimated 249 million malaria cases and 608,000 related deaths across 85 countries worldwide. The African Region bore the greatest burden, accounting for 94% of global malaria cases (233 million) and 95% of malaria deaths (580,000). Children under the age of five represented nearly 80% of all malaria-related deaths in the Region. The use of mathematical models to study malaria transmission was first pioneered by Ross (1911), who described the interactions between humans and mosquitoes through a system of ordinary differential equations (ODEs). This work was later extended by MacDonald (1957), who introduced important concepts such as the basic reproduction number, R_0, the influence of mosquito biting rates, and the duration of the infectious period, thus providing a more comprehensive framework for analyzing malaria transmission dynamics. The study indicated that

$$R_0 = \frac{m\, a^2\, \rho^n\, \beta_h\, \beta_m}{\mu_m\, \mu_h}$$

where m is Mosquito-to-human ratio, a^2 is biting rate, ρ^n Probability of mosquito survival through the extrinsic incubation period (EIP), β_h is transmission probability from mosquito to human per bite, β_m is transmission probability from human to mosquito per bite, μ_m is mosquito death rate and μ_h is human recovery. Where R_0>1 indicates malaria spread guiding control strategies.

Ngwa and Shu (2000) developed and analyzed a Susceptible - Exposed - Infectious - Recovered - Susceptible (SEIRS) model to investigate malaria transmission dynamics between human and mosquito populations. Their study introduced the threshold parameter, the basic reproduction number (R_0), demonstrating that malaria persists when $R_0 > 1$, whereas the Disease-Free Equilibrium (DFE) is locally stable when $R_0 < 1$ and globally stable for $R_0 \leq 1$. These findings, supported by numerical simulations, provide a useful framework for assessing malaria control strategies.

Mukhtar *et al*. (2018) examined the impact of bed net coverage on malaria transmission in South Sudan and found that greater use of bed nets significantly reduced malaria incidence. The study considered factors like population density, seasonal mosquito abundance, and bed net effectiveness. The study concluded that widespread distribution of insecticide-treated bed nets, along with other control measures, can effectively reduce malaria transmission in high-risk areas.

Agusto *et al*. (2012) investigated the influence of bed net usage on malaria prevalence by developing and analyzing a basic Susceptible-Infectious (SI) model that incorporates interactions between human and mosquito populations. The study explored the role of human behavior, particularly the inadequate or ineffective use of mosquito nets, in facilitating malaria transmission. The analysis revealed the presence of a backward bifurcation, suggesting that merely reducing the reproduction number is insufficient to eliminate the disease unless the initial number of infections in both populations is considerably large.

Chitnis *et al*. (2006) conducted a bifurcation analysis of a mathematical model for malaria transmission, emphasizing the significant role of backward bifurcation in shaping disease dynamics. Their findings demonstrated that lowering the basic reproduction number below unity does not necessarily ensure malaria eradication, as multiple endemic equilibria may still exist. The study underscored the importance of integrated control measures, including the use of mosquito nets, indoor insecticide spraying, and prompt treatment of infected individuals, to effectively reduce malaria prevalence and achieve disease elimination.

Mbogo *et al*. (2018) proposed a stochastic model to investigate malaria transmission dynamics, emphasizing the influence of random factors on disease spread and treatment outcomes, especially in regions with low transmission rates. Despite advances in control strategies, challenges such as drug resistance and inconsistent treatment adherence continue to hamper eradication efforts. This model provides valuable information on the effectiveness of interventions and the potential for malaria elimination. The models mentioned earlier did not consider the specific challenges of malaria transmission and treatment in conflict zones. Although there is a clear need to model malaria dynamics and treatment in these areas, very little focus has been given to developing such specialized models. This study aims to ensure there is effective treatment of humans by considering full treatment for individuals and under dose treatment in case of conflict zones.

1.2 Statement of the Problem

Malaria remains among one of the deadliest infectious diseases globally, continuing to cause critical illness and numerous fatalities annually, especially affecting children and pregnant women in sub-Saharan Africa. Despite extensive global control measures; including the application of insecticide-treated bed nets, indoor residual spraying, preventive therapies, and improved diagnostic and treatment programs, the disease still poses a major public health concern. The persistence of malaria in numerous endemic regions suggests that existing control measures do not have uniform effectiveness everywhere, especially in regions disrupted by social and political instability. These challenges highlight the necessity for more comprehensive approaches to understanding malaria dynamics in complex settings. Mathematical modeling has played a crucial role in explaining malaria transmission patterns and in assessing the impact of various control interventions. Many studies have focused on spatial transmission, seasonal variations, cost-effectiveness, drug resistance, and climate effects. However, limited attention has been given to modeling malaria in areas affected by conflict, where instability, displacement, and destruction of health facilities severely hinder effective treatment and prevention. In such environments, full treatment is often difficult to achieve, leading to partial or incomplete therapy that sustains infection and encourages drug resistance. Hence, this study aims to develop a mathematical model that describes malaria transmission and

treatment: a case in conflict zones, incorporating both full and partial treatment scenarios. The model clarifies how conflict conditions intensify malaria transmission and to assess the efficiency of interventions designed for these high-risk population.

1.3 Objectives of the Study

1.3.1 Main Objective

The primary goal of the study is to develop and analyze a general model for Malaria transmission and treatment: a case in conflict zones.

1.3.2 Specific Objectives

The detailed objectives of this study are:

i. To develop Mathematical model of malaria in conflict zones.

ii. To perform stability analysis of the model.

iii. To conduct sensitivity analysis to determine the parameters that increases the spread of malaria.

iv. To perform numerical simulations of the model to validate analytical results and determine the spread of malaria in conflict zones.

1.4 Significance of the Study

Proper management of malaria in conflict areas is crucial for reduce mortality and transmission, especially given the limited health resources in these areas. Enhancing access to treatment can lead to better health outcomes and address the challenges associated with displacement and weakened health systems. Understanding the spread dynamics of malaria within conflict areas enables focused intervention strategies that can protect lives and control the spread of the infection. In stable regions, effective treatment is also essential to prevent re-emergence and reduce transmission. The goal of this study is to minimize transmission of malaria a case in conflict zones by ensuring full treatment, suboptimal treatment of individuals in conflict-affected areas.

1.5 Operational Definition of Terms

This study will utilize several key terms, which are defined in the corresponding section.

Basic Reproduction Number : The Basic Reproduction Number is a key concept in epidemiology that indicates the average number of new infections caused by one infected person in a fully susceptible population throughout the period of disease transmission.

Conflict zones: Conflict zones are regions experiencing ongoing or recent armed conflicts, wars, or widespread violence that disrupts governance, social structures, and public safety. These zones are often characterized by political instability, insecurity, and humanitarian crises, including displacement, loss of lives, and destruction of infrastructure. Conflict zones may involve state actors, non-state groups, or a combination of both, leading to complex situations where essential services like healthcare, education, and access to food and water are severely compromised. Such areas pose significant challenges for development, peacebuilding, and the protection of vulnerable population.

Epidemic: An epidemic is characterized by the swift transmission of a contagious disease affecting a large number of individuals in a particular geographic region over a short timeframe. It usually occurs in populations with limited immunity to the disease, leading to an unusually high number of cases. Epidemics can be triggered by viruses, bacteria, or other pathogens, and their severity depends on factors such as the disease itself, the immunity of the population, and the effectiveness of public health interventions.

Epidemiology: Epidemiology is the scientific discipline that examines the distribution and causes of health-related events or conditions within specific populations, and applies this knowledge to manage and prevent health issues. It aims to understand the patterns, origins, and impacts of diseases by studying various factors such as exposure, behavior, environment and genetics. By identifying risk factors and protective measures, epidemiology provides the foundation for public health interventions, disease prevention, and health policy development, aiming to improve population health and reduce the burden of diseases.

Full treatment: Full treatment refers to a comprehensive medical intervention aimed at effectively eradicating a disease or its symptoms through the complete administration of prescribed therapies. In the case of malaria, treatment entails completing a full regimen of antimalarial medications, like artemisinin-based combination therapies (ACTs), adjusted according to the patient's age, weight, and overall health condition. Full treatment ensures adherence to medication, addresses complications such as fever or organ damage, and includes follow-up care to prevent relapse or reinfection. Additionally, it encompasses access to proper diagnosis and healthcare services to maximize recovery and reduce transmission risk.

Malaria: Malaria is a parasitic illness caused by Plasmodium species and is transmitted to humans through the bites of infected female Anopheles mosquitoes. After entering the bloodstream, the parasite travels to the liver, where it multiplies before infecting red blood cells. This infection causes symptoms such as fever, chills, headache, fatigue, and in severe cases, can lead to organ failure or death. Malaria is most common in tropical and subtropical areas, especially in sub-Saharan Africa, South Asia and parts of South America. Although it is preventable and treatable through methods like insecticide-treated bed nets, antimalarial medications, and mosquito control efforts, malaria continues to pose a major global health challenge, particularly in areas with limited resources.

Non-conflict zones: Non-conflict zones are regions that are not experiencing active armed conflicts, widespread violence, or political instability. These areas are generally characterized by peace, stability, and functioning governance, allowing for the normal operation of social, economic, and political systems. In non-conflict zones, essential services such as healthcare, education, and infrastructure are typically accessible and maintained, enabling communities to thrive without the immediate threat of violence or displacement. These regions often provide a conducive environment for development, investment, and the protection of human rights.

Numerical simulation: Numerical simulation refers to the use of computational algorithms and mathematical models to approximate and analyze the behavior of complex systems that cannot be solved analytically. It involves discretizing continuous models, such as differential equations, into a form that can be computed on a digital computer. Numerical simulations are commonly employed across disciplines like physics, engi-

neering, economics, and biology to forecast results, optimize systems, or explore phenomena that are challenging to observe firsthand. The precision of these simulations relies on factors including the selected method, step size, and available computational power.

Susceptible: Susceptible refers to individuals or populations that are at risk of contracting a disease or infection because they have not yet been exposed to the pathogen and lack immunity, either through prior infection or vaccination. These individuals are vulnerable to becoming infected upon contact with the infectious agent. The size of the susceptible population is crucial in the dynamics of disease transmission, as it represents the group of individuals who can potentially become infected and help propagate the disease.

Under-dose treatment: Under-dose treatment refers to the administration of a medication or therapeutic intervention at a dosage lower than the recommended or effective level required to achieve the desired therapeutic outcome. This can occur due to errors in prescription, patient non-compliance, and inadequate access to medication, or intentional dose reduction by healthcare providers. Taking doses below the recommended level can result in ineffective treatment, allowing the disease or infection to continue or worsen. In infectious diseases, this can also promote drug resistance, as pathogens are exposed to drug levels that are too low to eliminate them. Ensuring appropriate dosing is critical for effective treatment and to prevent complications or resistance.

CHAPTER TWO

LITERATURE REVIEW

2.1 Epidemiological Models

Sir Ronald Ross. (1911), formulated the first mathematical framework of malaria transmission, which provided a quantitative framework for understanding and controlling the disease. His work connected how mosquito population fluctuations influence malaria spread within human populations, introducing the now-critical concept regarding the basic reproduction number R_0 measure of how many the infections resulting from a single infected individual within a fully susceptible population. Ross's model also explored the threshold density of mosquitoes, identifying the minimum population level required to sustain disease transmission.

By demonstrating that reducing mosquito density below this threshold could effectively interrupt malaria transmission, Ross highlighted the importance of vector control measures, such as draining stagnant water to eliminate breeding grounds and using insecticides. These foundational models marked the beginning of mathematical epidemiology, inspiring subsequent developments in disease modeling. Ross's approach not only transformed malaria research but also influenced an assessment of other infectious diseases, paving the way for the application of mathematical tools in public health interventions and policy-making.

Macdonald. (1957) refined the Ross-Macdonald malaria transmission model by introducing additional parameters that enhanced the understanding of host-vector interactions. Specifically, he incorporated mosquito biting rates, which represent the frequency at which mosquitoes feed on human blood, and human recovery rates, which capture the speed at which infected individuals recover. These refinements allowed for a more precise calculation of the basic reproduction number and highlighted the essential role of vector dynamics, human infectivity, and the duration of infectiousness in shaping malaria transmission.

Aron. (1988) studied the dynamics of malaria immunity using mathematical models, focusing on how immunity develops with repeated exposure and impacts transmission. The study analyzed age-structured models that incorporated various immunity functions, such as reducing susceptibility to symptomatic disease, improving recovery rates,

and regulating parasite densities. The study contributed to knowledge on the observed decline in parasitaemia and clinical cases with age, helping to explain the complicated interplay between immunity and the dynamics of malaria spread.

Smith *et al*. (2006) formulated mathematical models to assess how malaria vaccines influence the epidemiology and progression of *Plasmodium falciparum*. These models incorporated vaccination into the Susceptible-Infectious-Recovery framework, accounting for waning immunity, vaccine efficacy, and age-specific dynamics, particularly in children under five.

Koella and Antia (2003) developed mathematical models to explore the emergence and transmission of drug-resistant malaria parasites. Their analysis examined how factors such as drug usage, treatment efficacy, and the fitness costs associated with resistance influence the dynamics of resistance development. The study also assessed the potential effects of different intervention approaches, including combination therapies and drug rotation, on limiting the spread of resistance. This work aimed to enhance understanding of the implications of anti-malarial drug use and support the design of strategies to prevent the proliferation of resistant malaria strains.

2.1.1 SEIR and SI Model

Anderson and May (1991) presented the Susceptible-Exposed-Infectious-Recovered (SEIR) model, a foundational tool in epidemiology for analyzing the transmission dynamics of infectious diseases, including malaria. The SEIR framework categorizes the population into four distinct groups: susceptible (S), exposed (E), infectious (I), and recovered (R). This compartmental structure is especially effective for modeling infections like malaria.where individuals' progress through different stages of infection and transmission is influenced by human and vector populations.

Kermack *et al*., (1927) introduced the Susceptible–Infected (SI) framework as an essential instrument in the study of disease patterns for understanding infectious disease dynamics. This model categorizes the population into two groups: individuals who are vulnerable to infection, and infected individuals, who have the disease as well can spread it to those who are susceptible.

Tatem *et al*., (2012) explored the impact of urbanization and malaria recession, using a SEIR model to assess how factors such as urban density, sanitation, and healthcare access influence malaria prevalence in both urban and rural settings. Their findings indicated that urbanization has generally contributed to a global decline in malaria transmission, largely due to improvements in public health infrastructure, sanitation, and vector control efforts. However, they also identified that rapid, unplanned urbanization, particularly in sub-Saharan Africa, has exacerbated malaria transmission in certain urban areas, underscoring the complex and context-dependent relationship between urban growth and malaria dynamics.

2.1.2 Malaria

Alhaj and Nyabadza. (2025) developed a compartmental model describing malaria transmission dynamics in conflict-affected regions, integrating parameters that capture the effects of armed conflict on disease transmission and healthcare access. The model considered how violence-induced disruptions influence mosquito–human interactions, treatment coverage, and intervention efficacy. Through stability analysis and sensitivity evaluation, the study showed that the basic reproduction number significantly increases when intensity raises conflict, highlighting the deteriorating public health infrastructure during war. Using data from Nigeria, Sudan, and the Democratic Republic of Congo (DRC), their results underscore the need for targeted control interventions that remain resilient under conflict conditions.

Yu *et al*. (2024) explored the interaction between violent conflict, climate variability, and malaria transmission risk in sub-Saharan Africa using a hybrid data–driven modelling approach. Although not purely a compartmental model, the study employs spatial spillover analysis and regression-based modelling to quantify how violent conflicts amplify malaria risk, particularly under climatic stress. The research demonstrated that violent events intensify malaria transmission through the breakdown of health systems, reduction of vector control, and population displacement. This quantitative link between armed conflict and increased malaria burden supports the inclusion of conflict variables in predictive malaria models.

Li *et al*. (2018) examined mobile population dynamics as a key driver of malaria vulnerability along the China–Myanmar border, a region historically influenced by political instability and cross-border conflict. Their model incorporates mobility-driven importation and reintroduction of malaria cases into low-transmission areas. Using stochastic simulations, they demonstrated how migrant and displaced populations can undermine malaria elimination efforts by sustaining low-level transmission. Although the study focuses on border mobility rather than direct conflict, its framework is highly relevant to modelling displacement-induced malaria spread in conflict zones.

WHO. (2023) identifies five species within the parasites of the genus *Plasmodium*, causing malaria in humans: *Plasmodium falciparum*, the most common as well lethal, responsible for majority of malaria-related deaths globally; Plasmodium vivax, recognized for its capacity to stay inactive in the liver and cause repeated occurrences Plasmodium *malariae*, which can cause long-lasting infections if untreated; Plasmodium ovale, less common but capable of causing relapses similar to P. vivax; and Plasmodium knowlesi, primarily affecting Southeast Asia and capable of causing severe disease.

Dondorp *et al*.(2010) discussed management of severe malaria, emphasizing introduction concerning intravenous an antimalarial medication as a superior treatment compared to quinine in severe cases. The study highlighted clinical trial data demonstrating decreased mortality rates with artesunate, particularly in resource-limited settings. Additionally, the authors recommended supportive treatments, such as blood transfusions and metabolic management, to address complications like severe anemia and hypoglycemia. The study concluded with a call for strengthening hospital capacity to ensure effective treatment of severe malaria.

White *et al*. (2018) reviewed policy implementation and the role of Artemisinin-Based-Combinations (ACTs) in national malaria control programs. The study outlined the successes of ACTs in reducing Plasmodium falciparum infections and explored their integration with preventive measures, such as insecticide-treated nets (ITNs). The study emphasized the importance of adhering to treatment guidelines and monitoring resistance patterns. They also highlighted the need for regular updates to national policies based on surveillance data to ensure continued effectiveness of malaria treatment programs.

Carter *et al*.(2021) explored advances in antimalarial drug development, focusing on next-generation therapies to address the growing challenge of artemisinin resistance. The study highlighted the mechanisms of action of ACTs and reviewed novel compounds under development, such as those targeting dormant liver-stage parasites. Carter *et al*. (2021) emphasized the importance of continued research and development to sustain progress in malaria treatment. They further emphasized the necessity for intergovernmental collaboration, researchers, and pharmaceutical companies to ensure equitable access to new treatments.

Traoré Bakary *et al*. (2018) developed a mathematical representation to study Malaria propagation within an environment with periodic fluctuations, accounting for mosquito age structure and variable biting rates. The model classifies humans into non-immune and semi-immune groups and examines stability of disease-free and endemic states by employing the reproduction number. Study highlights that controlling malaria depends on reducing below one and validates results through numerical simulations.

Collins and Duffy, (2022), presented a mathematical framework for studying malaria transmission, focusing on drug resistance and treatment dynamics in Nigeria. They modeled the interactions between humans, mosquitoes, and different types of malaria (resistant and susceptible). The study incorporated treatment failure rates, bed net use, and drug-resistant strains into the transmission dynamics. The authors used the model to analyze steady states and the basic reproduction number, which offers understanding of how interventions such as bed nets and treatment strategies can affect malaria transmission and resistance.

Githeko, (2007) studied environmental factors influencing malaria transmission in Kenya, focusing on elements such as temperature, rainfall and vegetation. The study found that high temperatures, seasonal rainfall and the availability of standing water significantly encourage the proliferation of malaria in tropical regions. In addition, increased rainfall provides suitable conditions for *Anopheles* mosquito populations, increasing the chance of contracting malaria transmission. The findings highlight the complicated interplay involving environmental and climatic elements contributing for the spread of malaria within sub-Saharan Africa.

Miller *et al*. (2008) describe the stages in the life history of *Plasmodium* species, parasites responsible pertaining to malaria, which includes two hosts: a human along with a female *Anopheles* mosquito. The parasite alternates between an asexual development phase within humans and a sexual phase within mosquitoes.

Centers for Disease control and prevention (2022) studied the asexual the developmental cycle of the malaria, which is triggered when an infected during a blood meal, a female mosquito introduces sporozoites into the bloodstream. These sporozoites then move to the liver, where they infect live by cells and undergo asexual replication, transforming into merozoites. Merozoites emerge into bloodstream as well infect in the red blood cells (RBCs), where they transform into trophozoites, which develop into schizonts. These schizonts rupture the infected RBCs rupture, freeing more merozoites that infect other RBCs, perpetuating the cycle. This process causes the fever and anemia related to malaria due to RBC destruction. Merozoites differentiate to gametocytes the reproductive form of the parasite, completing cycle as well as enabling transmission.

Carter Center, (2018) stated that species like Plasmodium vivax and Plasmodium ovale have a unique ability to produce inactive stages known as hypnozoites, which remain in the liver and can reactivate following several months or even years afterward, causing relapse infections. Such characteristic makes these species particularly difficult to eradicate, as they can evade treatment aimed at the blood stage of the parasite.

CDC, (2020) investigated the lifecycle of Plasmodium, detailing how gametocytes are consumed by a mosquito from an infected human host. These gametocytes undergo reproduction through fusion of gametes within mosquito, forming a zygote developing into motile ookinete. The ookinete subsequently passes through the mosquito's gut wall and develops into an oocyst, within which numerous sporozoites develop. These sporozoites subsequently are discharged and move to the mosquito's salivary glands, prepared to infect a new human host during the subsequent blood meal.

2.1.3 Epidemiology of Malaria

Greenwood, (1997), highlighted epidemiology such as Malaria as a burden, especially across sub-Saharan Africa, where children and expectant mothers are most affected. He emphasizes the importance of climatic conditions, transmission dynamics, as well as

partial how immunity affects the disease's spread. Challenges include drug-resistant Plasmodium, insecticide-resistant mosquitoes, and weak health systems, necessitating integrated control strategies.

Autino *et al*.(2012), Studied Malaria distribution and dynamics in endemic areas, discussed that malaria accounted for significant morbidity and mortality worldwide, with the disease predominantly impacting children below five years and expectant mothers. WHO,(2010), around 216 million reported malaria cases and 655,000 deaths occurred worldwide, most with the majority occurring in sub-Saharan Africa. Plasmodium vivax , more widely distributed outside Africa especially in regions such as Southeast Asia, Latin America, and the Western Pacific, largely due to higher adaptability as well as its vector mosquitoes to diverse ecological settings.

Bhatt *et al*.(2015), Studied outcome of *Plasmodium falciparum*, intervention measures across Africa from 2000 to 2015and found that socio-economic factors, particularly poverty, increase vulnerability to malaria through limited ability to obtain prevention, diagnostic evaluation and therapy. Poor infrastructure, inadequate medical care, lack of resources exacerbates the impact of the disease. Targeted interventions, such as subsidizing preventive tools and strengthening health systems, are essential to reduce malaria transmission and improve outcomes in low-income areas.

Paaijmans *et al*.(2010) studied effects of climatic conditions, such as temperature, rainfall, and humidity, on malaria dynamics. These environmental conditions influence the longevity and reproductive capacity of Anopheles mosquitoes, the vectors of malaria. In favorable climates, malaria transmission may take place across the year, while in less favorable areas it is seasonal. The study highlighted the importance of exploring the link between climate and malaria for prediction of outbreaks as well as the planning of control measures, particularly considering climatic conditions change, which may alter modes of transmission.

Conway, (2007) studied the molecular epidemiology of malaria, focusing on the genetic dynamics of *Plasmodium* parasites and *Anopheles* mosquitoes. Malaria, which mainly affects sub-Saharan Africa, is transmitted by mosquito bites, causing symptoms such as fever and anemia. Environmental factors and socioeconomic conditions influence

transmission, with pregnant women and children particularly vulnerable. Control measures, including insecticide-treated beds, indoor spraying, and antimalarial drugs, have advanced, and the RTS,S/AS01-malaria vaccine shows promise.

2.1.4 Control of Malaria

WHO, (2022) states that mosquito nets treated with insecticide (ITNs), especially long-lasting mosquito nets treated with insecticide (LLINs)are most effective interventions to reduce disease transmission. Since 2000, more than 2 billion of LLINs have been distributed worldwide, significantly reducing human-mosquito contact and contributing to a decline in malaria cases. LLINs ensure there is a barrier as well as chemical defense preventing mosquito bites, making them a cornerstone of malaria prevention. Indoor residual spraying (IRS) , endorsed by WHO is essential parasite eradication measure, especially in areas of intense malaria transmission. Regular indoor application of insecticides reduces the population of malaria-carrying mosquitoes and interrupts disease transmission. These interventions are a key component of WHO malaria reduction and elimination efforts, strategies aimed at reducing the global consequences of the disease.

Ashley *et al*.(2014), investigated the occurrence of artemisinin resistance in *Plasmodium falciparum* malaria and identified that the resistance is largely due to genetic alterations in the K13 genetic sequence, such as R539T and C580Y. These mutations result in longer parasite clearance times, reducing the effectiveness of ACT. This treatment non-responsiveness issue especially critical, Southeast Asia, where the spread of resistant strains threatens malaria control initiatives. The study emphasizes the necessity for ongoing monitoring of resistance patterns to ensure the continued efficacy of existing treatments.

WHO, (2019) investigated Malaria vaccine: RTS,S/AS01 malaria vaccination pilot program. The RTS,S/AS01 vaccine against malaria was launched during 2019 as part of a pilot program in Ghana, Malawi and Kenya. This vaccine complements existing malaria intervention measures, including mosquito nets treated with insecticide and antimalarial drugs. The introduction of RTS,S has demonstrated the ability to decrease the number of malaria cases and serious outcomes among under-five children, making it an essential tool for malaria prevention, particularly in areas of high transmission. The program has

demonstrated the impact of vaccination on lowering the burden associated with malaria, along with other preventive measures.

Monroe *et al*.(2021) studied *World Malaria Report* and found that malaria control strategies, including insecticide-treated nets (ITNs), indoor residual spraying (IRS), and preventive therapies, seasonal malaria chemo-prevention (SMC), have significantly decreased malaria cases as well as severe outcomes among children under five. These interventions lower transmission and decrease the severity of the disease, particularly among young children vulnerable to complications such as severe anemia and cerebral malaria. Combination use of these measures which cause notable decreases of malaria-related incidence of disease and related deaths in high-risk areas.

Wongsrichanalai *et al*. (2007) studied a review of Malaria diagnostic tools, highlighted quick diagnostic methods tests (RDTs) in combating malaria, particularly in regions with limited access to microscopy. The study emphasized that RDTs offer quick and accurate results that enable timely treatment and help reduce malaria transmission. While RDTs enhance disease detection and aid in lowering morbidity and mortality when used with proper treatment, the study pointed out potential limitations, including false positive and negative results that may impact treatment effectiveness. Nevertheless, RDTs are considered a crucial asset in the malaria fight, especially in remote areas with inadequate healthcare facilities.

Menéndez *et al*. (2010), studied on Intermittent Preventive Treatment during pregnancy and reduced neonatal mortality and showed that infectious parasitic prevalence test with sulfadoxine-pyrimethamine (SP) significantly reduces neonatal mortality by reducing malaria infections, anemia and risks such as low birth weight. IPTP is a critical part of the fight against malaria, improving maternal and neonatal health outcomes. Alongside mosquito nets with insecticidal treatment as well as rapid treatment, it contributes to lowering the burden of malaria, although challenges such as drug resistance highlight the need for continued innovation in prevention and treatment.

Fatmaningsih *et al*. (2024) investigated advances in the fight against malaria: a new era of innovations in treatment and vector control and highlighted new strategies to fight malaria, focusing on the long-acting drug tafenoquine to prevent relapse of Plasmodium

vivax and on genetically modified mosquitoes to combat insecticide resistance. These innovations, together with improved regulatory processes and preparedness of health systems as a key to accelerating efforts to fight malaria, in line with the WHO global strategy to improve malaria prevention and treatment.

2.1.5 Mathematical Modeling of Malaria Treatment

Anderson *et al*.(1992), formulated a mathematical framework for malaria transmission using Susceptible-Infected-Recovered (SIR) framework, classifying the human population into susceptible, infected, and recovered compartments. The framework also includes mosquitoes as vectors, with susceptible and infected compartments. Key considerations such as infection rates and delay periods for humans as well as mosquitoes, and partial body's defense mechanism are included. The study highlighted the fundamental contribution of vector management strategies, vector control interventions drugs, which provide valuable information effectiveness of control interventions effectiveness of various management measures.

Keeling and Rohani (2008), in Modeling Infectious Diseases in Humans and Animals, discussed SEIR framework, which includes an exposed (E) category to account for the incubation duration of diseases, making it particularly relevant for modeling malaria and the life cycle of the Plasmodium parasite. While not the model's originators, they emphasized its effectiveness in capturing disease dynamics and enhancing the realism of transmission models, highlighting its adaptability to complex epidemiological contexts.

Hoshen *et al*. (2001) studied a pharmaco-kinetics and pharmaco-dynamics model of mefloquine activity in humans, focusing on the integration of the drug's absorption, distribution, metabolism, and excretion with its effects on malaria parasites. Their model linked plasma concentration to parasitemia clearance, providing a framework to predict treatment outcomes. The study also addressed the potential development of drug resistance, offering insights into optimizing mefloquine dosing regimens to enhance efficacy and manage resistance in regions where malaria is consistently present.

Dondorp *et al*. (2010) emphasized the usefulness regarding PK-PD models in clinical trials, where they help simulate different dosing scenarios and predict treatment success. These models are crucial for optimizing drug dosing, improving efficacy, and anticipating drug resistance, particularly in malaria treatments.

Tchuence *et al*.(2011) developed a mathematical framework to study antimalarial medication resistance, examining its effects regarding the spread of malaria treatment. The model emphasized on treatment rates, drug efficacy, and resistance emergence in shaping disease dynamics, highlighting that strategies like combination therapies and improved treatment coverage are essential for controlling resistance and sustaining mitigation measures

Otieno *et al*. (2016) developed a mathematical framework to perform assessing the cost-effectiveness of different control measures for disease management .Study focused on evaluating various intervention measures, such as treatment, prevention, and awareness campaigns, to identify the leading cost-effective combination aimed at lowering disease incidence burden. Model incorporated key factors, including disease transmission dynamics, economic costs, and population-level health outcomes. By applying optimal control theory, they determined strategies that maximize the health benefits while minimizing associated costs, contributing meaningful analysis into healthcare policy and distribution of resources in Kenya.

Amadi, (2021) developed an applying an agent-based simulation to analyze the elaborate factors affecting malaria prevalence, including vector behavior, human mobility, and healthcare access. The model simulated localized disease control interventions, including the use of insecticide-treated nets and administration of antimalarial drugs, providing insights into effective malaria control strategies.

Rajnarayanan *et al*. (2024) investigated a data-driven mathematical representation of malaria distribution, integrating epidemiological data to validate and optimize control strategies like bed nets, spraying, and treatment. The study emphasized the role of environmental factors and pointed out the necessity of tailored measures within endemic regions, demonstrating about the usefulness of data-driven approaches in disease management.

2.1.6 Equilibria, Stability and Sensitivity Analysis

Hethcote, (2000), has shown that infectious disease modeling, equilibrium points play a critical role in understanding the long-term dynamics of diseases. Equilibrium is classified categorizing the model into disease-free equilibrium (DFE) and endemic equilibrium (EE). The DFE occurs under the condition that disease disappears, with no infected individuals in the population, while EE represents an equilibrium in which the disease remains present at a constant degree in the population. These concepts are essential for analyzing the equilibrium and behavior regarding the transmission models.

Diekmann *et al*.(1990), introduced the fundamental reproduction rate, as a fundamental limit parameter in order to determine stability of these equilibria. If, the DFE is stable in the world or in the place, which implies that the disease will eventually disappear. However, if, DFE becomes unstable and EE appears, indicates the continuous transmission of the prevalence of disease among individuals.

Chitnis *et al*. (2008), further investigated basic reproduction number (R_0) by analyzing the influence of factors such as vector control and treatment. Study showed that these parameters can shift populations between the disease-free states (DFE) and the endemic state (EE), providing practical strategies for disease control.

Anderson and May (1991) focused regarding the significance of stability regarding the behavior of infectious disease spread, particularly malaria. They studied how stable equilibria allow a system to return to its initial state after small perturbations, such as a temporary increase in infection rates. The study noted that in the fight against malaria, effective treatments that rapidly reduce infection levels are essential to maintain the equilibrium state of the system, ensuring that the disease burden remains under control, and prevent large-scale outbreaks.

Dondorp *et al*.(2010) investigated and found that unstable equilibrium occurs when small changes lead to larger fluctuations, which is particularly concerning when drug resistance is increasing or access to treatment is limited. Several factors affect the stability of malaria treatment. High therapeutic efficacy promotes stability, ensuring effective infection management and outbreak prevention. Conversely, the use of monotherapy can destabilize treatment efforts, facilitating the occurrence of resistant strains of malaria.

Smith *et al*. (2007) analyzed the stability of malaria models under seasonal variations in transmission rates. They studied how equilibrium points can shift with seasonal changes in vector density, focusing on the steadiness of the endemic state over time. Their work showed that the degree to which the model reacts to changes in vector control interventions can vary considerably between seasonal periods.

Kiszewski *et al*. (2004) contributed to the insights into how malaria spreads and progresses equilibrium by focusing the influence of the spatial heterogeneity and population movements. Their work has highlighted that the stability of malaria equilibrium can vary considerably in regions with different transmission intensities and different levels of population immunity. Sensitivity analysis has shown that localized interventions can have variable effectiveness depending on spatial distribution

2.1.7 Numerical Simulation

Tumwiine *et al*.(2008) introduced a malaria model focusing on protective interventions among high-risk populations, including travelers, migrants, and residents entering endemic regions. The study formulated a system of nonlinear ODEs and analyzed threshold conditions for malaria persistence using the next-generation matrix method. They used numerical simulations to examine how prophylactic measures and vector control among immigrants affect malaria transmission levels. Simulation results showed that increasing the proportion of individuals using protective interventions; such as mosquito repellents and chemoprophylaxis, significantly reduces infection rates, especially when high-risk populations are mobile. Although the study was carried out under general public health conditions, its findings are highly relevant to conflict contexts, where population displacement and migration resemble the movements of non-immune travelers entering endemic regions. By replicating these mobility patterns through simulation, the study demonstrated how human movement during conflict can alter local malaria dynamics, stressing the importance of preventive strategies for displaced populations.

Sedda *et al*.(2015) explored the statistical relationship between armed conflict and malaria prevalence using a geostatistical simulation approach. Drawing on data from 1997 to 2010 across several African countries, they developed a spatial model that combined conflict event records with Plasmodium falciparum prevalence maps. Using mixed-

effects regression and Monte Carlo simulations, they quantified the spatial and temporal association between conflict frequency and malaria intensity. The simulations revealed that areas within close proximity to conflict events recorded higher malaria prevalence than those further away, largely due to the collapse of health infrastructure, halted mosquito control programs, and increased human exposure in refugee settlements. The study concluded that armed conflict is a major determinant of malaria transmission patterns in Africa, not merely through environmental effects but also by disrupting preventive and treatment measures. Their work illustrates how simulation can merge epidemiological and geospatial data to forecast malaria resurgence in fragile settings, offering a blueprint for integrating conflict variables into disease modeling.

Wedajo *et al*. (2020) constructed a deterministic SEIRS malaria model that integrates human treatment and immunity loss into the transmission framework. Their model divided the population into susceptible (S), exposed (E), infectious (I), treated (T), and recovered (R) classes, linked to corresponding mosquito compartments. The researchers derived both the disease-free and endemic equilibria and performed a stability analysis using the basic reproduction number. They then applied numerical simulations using the Runge–Kutta method to study the temporal evolution of infection levels under different treatment rates. The simulation graphs revealed that increasing the treatment rate substantially decreases infection prevalence, while low treatment or delayed medical attention allows the disease to persist at endemic levels. Although their model was not originally developed for conflict conditions, its structure provides a strong basis for adapting simulation experiments to unstable regions. In conflict zones where treatment access is inconsistent, simulations of this type can quantify how partial compliance or medication shortages influence infection resurgence and recovery dynamics.

Alhaj and Nyabadza. (2025) developed a deterministic compartmental model to analyze malaria transmission dynamics in regions affected by armed conflict. Their model incorporated both human and mosquito populations, subdividing the human population into susceptible, exposed, infectious, treated, and recovered compartments. What distinguished their work from earlier malaria models was the inclusion of conflict-related parameters that modify transmission and recovery rates. Specifically, they simulated the effects of disrupted healthcare systems, reduced access to insecticide-treated nets, and

increased human exposure to mosquito bites. The study employed numerical simulations using a fourth-order Runge–Kutta method to approximate the solutions of the nonlinear differential equations. The results showed that when conflict intensity increases, malaria prevalence rises sharply due to limited treatment availability and weakened preventive measures. They further observed that the basic reproduction number exceeds unity under severe conflict scenarios, making elimination nearly impossible without targeted interventions. Their simulations highlight the urgent need for conflict-sensitive malaria control strategies, such as mobile treatment units and emergency distribution of vector control tools, to reduce the disease burden in unstable regions.

CHAPTER THREE

METHODOLOGY

3.1 Model Description and Formulation

3.1.1 Model Formulation

The framework is derived from SEIR and SIR frameworks described in 2.2. The population under consideration is N, The model is designed to analyze the dynamic interactions considering interactions between humans and mosquitoes over time t. The human host population enters the susceptible compartment of humans (S_H), entering the exposed class (E), treatment of infectious humans a case in conflict zones (I_C), infected individuals in other zones (I_F), full treatment of humans in conflict zones (T_P), under dose treatment of humans in conflict zones (T_n) and recovered humans (R), and that of mosquitoes into two divisions: Susceptible vectors (S_V) along with mosquitoes in the infectious class (I_V). These are main features of the model; π is recruitment within the susceptible human population, μ death rates of susceptible class, α represents the infection rate among humans, λinfectious rate to full treatment humans, θ is natural deaths rates of full treatment humans, ε is death rates infected humans in other zones, ω is treatment rate of infected of full treatment individuals, χ is recovery rate of full treated individuals, e is death rate of full treatment humans, γ is recovery rate of other zones individuals, τ is death rates of infectious mosquito, Ψ represents the mosquito infection rate, ν is represents the mosquito infection rate from other zones patients, ϕ is rate of infection of mosquitoes from infected humans in conflict zones, Λ is recruitment of susceptible mosquitoes, Z is rates of infected mosquito bites to susceptible humans and ρ is rate of recovered exposed humans. The $SEI_CI_FT_PT_nR-SI$ describes malaria transmission and treatment a case in conflict zones, incorporating human compartments for susceptible-exposed-infected in conflict zones and none conflict zones-full treatment and under dose treatment-recovered along with mosquito populations for susceptible-infected. This model captures the impact of malaria transmission and treatment a case of conflict zones, hence useful for studying malaria control in conflict regions.

3.1.2 Model Assumptions

i. Population size varies over time.

ii. Humans progress through stages of disease in a linear manner.

iii. Primary source of infection for humans is through mosquito bites, and that human-to-human transmission is considered a secondary route.

iv. Recovery rate for treated and exposed individuals are assumed to be fixed and do not vary based on individual health or treatment effectiveness.

v. Population is homogeneous.

vi. All people have equal chances of getting malaria.

3.2 Model Variables and Parameters

Table 1: Model Variables and their Description

Variable	Description
E	Exposed humans
I_C	Infectious population in conflict zones
I_f	Infectious individuals in conflict-free zones
I_V	Infectious mosquitoes
R	Recovered humans
S_H	Susceptible humans
S_V	Susceptible mosquitoes
T_n	Treatment of humans being compromised
T_P	Full treatment of humans

Table 2: Model Parameters and their Description

Parameter	Description
$\wedge$	Recruitment of vulnerable mosquitoes
e	Death rate of full treatment of humans
N	Total population
τ	Mortality rate of infectious mosquitoes
$\vee$	Rate of infection of mosquitoes from non-conflict zones
X	Recovery rate of full treatment humans
Z	Infected mosquito biting rates to susceptible humans
α	Infection rate for humans
γ	Recovery rate of humans in non-conflict zones
ϵ	Death rates of compromised humans
θ	Death rate of infected humans in conflict zones
λ	Infectious rate of humans in conflict zones
μ_m	Natural death rate of mosquitoes
μ_h	Natural death rate of humans
Π	Recruitment of susceptible humans through birth rate
ρ	Recovery rate of humans to become exposed to the disease
ψ	Infection rate of mosquitoes
ω	Treatment rate for infected humans undergoing full treatment
Φ	Infection rate of mosquitoes from non-conflict zones

3.2.1 Model Flow Chart

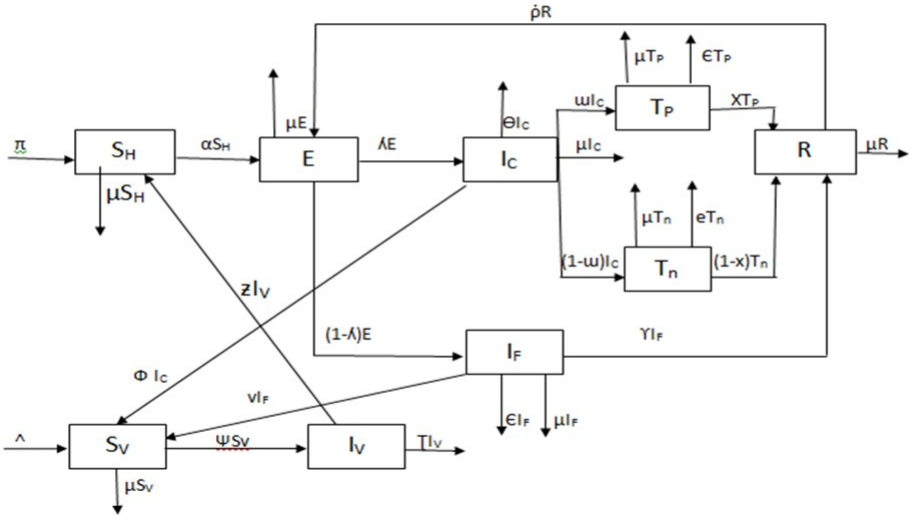

Figure 3.1: Model Flow Chart

3.3 Model Equations

The following equations are formulated based on the model flow diagram in figure 3.1, describing the interactions between the nine compartments, showing how individuals and vectors transition from one stage to another over time. These interactions are governed by biological, epidemiological and treatment related parameters used to analyze the spread of malaria and evaluating control strategies in conflict zones.

3.3.1 Human Population

Susceptible individuals (S_H) become exposed (E) upon being bitten by an infectious mosquito (I_V), occurring at a rate proportional to S_H. Exposed individuals (E) then progress to the infectious stage, I_C and I_F at a rate λE and $(1-\lambda)E$ respectively. Infected individuals in I_C and I_F progresses to full treatment T_P and partial treatment T_n. From T_P and T_n progresses to recovery compartment (R) which represents human population equations 3.1 to 3.7..

$$\frac{dS_H}{dt} = \pi + \mathbb{Z}I_V - \alpha S_H - \mu S_H \tag{3.1}$$

$$\frac{dE}{dt} = \alpha S_H + \rho R - \lambda E - (1-\lambda)E - \mu E \tag{3.2}$$

$$\frac{dI_C}{dt} = \lambda E - \phi I_C - \Theta I_C - \omega I_C - (1-\omega)I_C - \mu I_C \tag{3.3}$$

$$\frac{dI_F}{dt} = (1-\lambda)E - \nu I_F - \epsilon I_F - \mu I_F - \gamma I_F \tag{3.4}$$

$$\frac{dT_P}{dt} = \omega I_C - \epsilon T_P - \mu T_P - X T_P \tag{3.5}$$

$$\frac{dT_n}{dt} = (1-\omega)I_C - eT_n - \mu T_n - (1-x)T_n \tag{3.6}$$

$$\frac{dR}{dt} = xT_P + \gamma I_F - \rho R - \mu R + (1-x)T_n \tag{3.7}$$

3.3.2 Mosquito Population

Susceptible mosquitoes (S_V) become infectious (I_V) after biting an infected human host, occurring at a rate given by ψS_V, enabling further disease transmission. These form the mosquito population compartment and the two equations derived from there.

$$\frac{dS_V}{dt} = \wedge + \phi I_C + \nu I_F - \psi S_V - \mu S_V \tag{3.8}$$

$$\frac{dI_V}{dt} = \psi S_V - zI_V - \tau I_V \tag{3.9}$$

The force of infection for both humans along with mosquitoes is defined by equation 3.10;

$$\lambda = \frac{\beta\left(I_C + \eta_1 I_V + \eta_2 I_F + \eta_3 T_n + \eta_4 T_p\right)}{N} \tag{3.10}$$

Equation (3.10) describes the rate at which susceptible individuals contract the infection through interaction with infectious individuals, where β denotes: the transmission rate or contact rate, which measures how efficiently the disease is spread from infectious individuals to susceptible ones. η_1, η_2, and η_3: Weighting parameters that modify the influence of each group on the total force of infection, with each factor reflecting variations in levels of infectiousness; η_1 adjusts the infectiousness of individuals in other zones (I_F), which may differ from those in conflict zones (I_C); η_2 adjusts for individuals receiving partial treatment (T_n), who may still spread the infection but at a reduced rate compared to untreated individuals; and η_3 adjusts for individuals under full treatment (T_P), who might have a lower but non-zero infectiousness due to effective treatment.

3.4 Model Analysis

3.4.1 Basic Reproduction Number R_0

Anderson and May (1991), Studied Infectious Diseases of Humans: Dynamics and Control and examined the threshold reproduction number (R_0), fundamental concept of infectious mathematical epidemiology.. According to this study (R_0) represents the mean number of secondary infection arising from one infectious person within a population in which every individual is susceptible. The study shows that ifR_0>1, the pathogen is capable to invade and circulate in the population; conversely, if R_0<1, the infection cannot sustain itself and will ultimately die out.. Study further extended the concept to account for heterogeneities in populations and vector-borne diseases, emphasizing its critical role in designing public health interventions such as vaccination and control strategies.

Heffernan *et al*. (2005) highlighted the importance of Lowering the basic reproduction number(R_0), below unity is essential for controlling and ultimately eradicating infectious diseases. Accurate estimation of (R_0) is fundamental to developing efficacious interventions for high spread diseases like malaria, measles, and COVID-19.

In this study, the epidemiological threshold (R_0) for the system will be derived by applying the next-generation matrix method. This will involve estimating the Jacobian matrix evaluated at the disease-free equilibrium (DFE) system. The characteristic roots obtained from the next-generation matrix will be calculated using Mathematica software

to assess the behavior of the system around the disease-free equilibrium point as well as quantify the potential for disease spread.

3.4.2 Stability Analysis

The stability analysis aimed to determine the conditions under which malaria could either be eradicated or persist within a population. This was achieved by identifying the equilibrium points of the model, particularly the Disease-Free Equilibrium (DFE) and the endemic equilibrium. The DFE was analyzed by applying the next-generation matrix method introduced by van den Driessche and Watmough. (2002) to derive the basic reproduction number, denoting whether the disease will die out ($R_0 < 1$)or persist ($R_0 > 1$). The Jacobian matrix corresponding to the system was evaluated at the equilibrium points to determine the sign of the eigenvalues and thus establish local stability. This analysis provided the threshold conditions for malaria elimination providing understanding of how treatment effectiveness and transmission dynamics influence disease persistence in conflict settings.

3.4.3 Sensitivity Analysis

Sensitivity analysis was conducted to identify the model parameters with the greatest impact on malaria transmission and treatment outcomes. Local sensitivity indices were computed to determine how small changes in each parameter affected the basic reproduction number. Parameters with positive sensitivity values were identified as those that promote disease spread, while negative values indicated parameters that suppress transmission.

3.4.4 Numerical Simulation

Numerical simulations were performed to validate the analytical results and explore malaria dynamics under varying conflict conditions. The set of ordinary differential equations was numerically solved using Runge–Kutta methods implemented in Python and Mathematica. Simulations compared baseline (non-conflict) scenarios with conflict settings, where treatment coverage was reduced, partial treatment increased, and transmission rates adjusted to reflect weakened healthcare systems. The results demonstrated that when ($R_0 < 1$), infection levels declined to zero, confirming the stability of the DFE, whereas when ($R_0 > 1$), infection levels stabilized at an endemic equilib-

rium. Graphical outputs such as impact of malaria treated population over time were used to visualize the model's behavior, providing evidence on how strengthening treatment coverage and vector control could substantially reduce malaria transmission even under challenging conflict conditions.

CHAPTER FOUR

ANALYSIS, RESULTS AND DISCUSSION

4.1 Model Analysis

This part of this study are expected to examine positivity, boundedness, the feasible region along with the behavior of the existence and stability of equilibrium points as well as the derivation regarding the basic reproduction number of $SEI_CI_FT_PT_nR$-SI model. It also explores the occurrence of an endemic equilibrium state as well as analyzes threshold conditions with respect to either persistence or eradication of the infection. Additionally, it includes an investigation of the examination of the stability of the disease-free equilibrium, both locally and globally.

4.1.1 Positivity of Solution

We prove positivity by proving the theorem below.

Theorem 1: If $S_H(0)$, $E(0)$, $I_C(0)$, $I_F(0)$, $T_C(0)$, $T_F(0)$, $S_V(0)$, $I_V(0)$, $R(0)$ are positive, then the solutions $(S_H(t), E(t), I_C(t), I_F(t), T_C(t), T_F(t), S_V(t), I_V(t), R(t))$ in equations (3.1 – 3.9) are strictly greater than zero for all $t > 0$.

Proof: Let

$$t^* = \sup\Big\{t > 0 : \begin{matrix} S_H(t) > 0, & E(t) > 0, & I_C(t) > 0, & I_f(t) > 0, & \\ T_C(t) > 0, & T_f(t) > 0, & S_V(t) > 0, & I_V(t) > 0, & R(t) > 0 \end{matrix}\Big\},$$

such that $t^* > 0$. From equation (3.1), equation (4.1) is obtained.

$$\frac{dS_H}{dt} = \pi + \mathbb{Z}I_V - \sigma S_H - \mu S_H \geq \pi + \mathbb{Z}I_V - (\sigma + \mu)S_H \tag{4.1}$$

Since equation (4.1) is a linear ordinary differential equation of the form

$$\frac{dy}{dt} + p(t)y = q(t),$$

then the integrating factor is given by equation (4.2):

$$I(t) = e^{\int_0^{t^*} \mu\, ds} = e^{\mu t} \tag{4.2}$$

Multiplying equation (4.1) throughout by $I(t)$, we obtain equation (4.3).

$$e^{\mu t}\frac{dS_H}{dt} + \mu e^{\mu t} S_H = e^{\mu t}\left(\Lambda - \beta S_H I_V\right) \tag{4.3}$$

Simplifying equation (4.3) gives equation (4.4).

$$\frac{d}{dt}\left(e^{\mu t} S_H\right) = e^{\mu t}\left(\Lambda - \beta S_H I_V\right) \tag{4.4}$$

Integrating both sides of equation (4.4) over the interval $t = 0$ to $t = t^*$ gives equation (4.5).

$$\int_0^{t^*} \frac{d}{ds}\left(e^{\mu s} S_H(s)\right) ds = \int_0^{t^*} e^{\mu s}\left(\Lambda - \beta S_H I_V\right) ds \tag{4.5}$$

Evaluating the left-hand side and right hand side of equation 4.4 to obtain equation 4.5

$$e^{\mu t} S_H(t) = S_H(0) + \int_0^{t^*} e^{\mu s}\left(\Lambda - \beta S_H I_V\right) ds \tag{4.6}$$

Solving for $S_H(t)$ in equation (4.6) gives equation (4.7).

$$S_H(t) = \frac{S_H(0) + \int_0^{t^*} e^{\mu s}\left(\Lambda - \beta S_H I_V\right) ds}{e^{\mu t}} \tag{4.7}$$

Since $S_H(0) > 0$, using the initial value $t = 0$, we have: Also, $\Lambda - \beta S_H I_V$ remains positive and bounded. $e^{\mu t} > 0, \quad \forall\, t > 0$.

$Consequently, S_H(t) > 0, \quad \forall\, t > 0$. The solution remains non-negative throughout, $\forall\, t > 0$. Thus, $S_H(t)$ remains positive.

Similarly, following a similar approach for the remaining equations (3.2)–(3.9) confirms that the solutions preserve positivity. Hence, we deduce that

$$S_H(t),\ E(t),\ I_C(t),\ I_f(t),\ T_C(t),\ T_f(t),\ S_V(t),\ I_V(t), \text{ and } R(t)$$

are positive, $\forall\, t > 0$.

Thus, theorem 1 is proved.

4.1.2 Boundedness of Solutions

Theorem 2: Consider $N_H(t)$ and $N_M(t)$ as the total populations of humans and mosquitoes at any time t, respectively, determined by the system of equations (3.1)–(3.9) given

above. If the recruitment rates π and Λ are positive and the natural death rates μ and μ_M are strictly positive, then the total populations $N_H(t)$ and $N_M(t)$ remain bounded, $\forall\, t \geq 0$.

Proof: It is proven that boundedness of solutions considering total human and mosquito population separately.

Step 1: The entire human population is given by equation 4.8

$$N_H = S_H + E + I_C + I_f + T_P + T_n + R \tag{4.8}$$

Differentiating equation (4.8) with respect to t, the rate at which the human population varies is expressed as in equation 4.9:

$$\frac{dN_H}{dt} = \pi - \mu N_H \tag{4.9}$$

Integrating the differential equation 4.9 with respect to time gives the general solution for the total human population as described by equation 4.10:

$$N_H(t) = \frac{\pi}{\mu} + \left(N_H(0) - \frac{\pi}{\mu}\right) e^{-\mu t} \tag{4.10}$$

$$N_H(t) \leq \frac{\pi}{\mu}, \quad \forall\, t \geq 0.$$

Step 2: Total mosquito population (N_M). Let the total mosquito population be defined by equation 4.11:

$$N_M = S_V + I_V \tag{4.11}$$

Differentiating equation (4.11) and substituting from equations (3.8)–(3.9), the temporal variation of the total mosquito population is given by equation 4.12:

$$\frac{dN_M}{dt} = \Lambda - \mu_M N_M \tag{4.12}$$

Solving the linear differential equation 4.12 yields equation 4.13.

$$N_M(t) = \frac{\Lambda}{\mu_M} + \left(N_M(0) - \frac{\Lambda}{\mu_M}\right) e^{-\mu_M t} \tag{4.13}$$

$$N_M(t) \leq \frac{\Lambda}{\mu_M}, \quad \forall\, t \geq 0.$$

Therefore, we conclude that $N_H(t)$ and $N_M(t)$ remain bounded, $\forall\, t \geq 0$. Hence, proved.

Table 1: Model Parameters, Values, Units, and Sources

Parameter	Value / Unit	Source
Λ	80 mosquitoes/day	Mwangangi et al., (2013)
ρ	0.05 (1/day)	Assumed
N	10000	Mkubwa et al., (2020)
Ψ	0.3 (1/day)	Mwangangi et al., (2013)
τ	0.1 (1/day)	Mwangangi et al., (2013)
Ω	0.2 (1/day)	WHO, 2022
$\vee$	0.3 per bite	Chitnis et al., (2008)
Φ	0.3 (1/day)	Chitnis et al., (2008)
X	0.3 (1/day)	WHO, 2022
μ_H	0.000039 (per day)	WHO, 2022
Z	0.4 bites/day	Mwangangi et al., (2013)
μ_m	0.1 (per day)	WHO, 2022
α	0.3 (1/day)	Chitnis et al., (2006)
Π	0.00006849 (1/day)	Chitnis et al., (2008)
γ	0.2 (1/day)	WHO, 2022
ϵ	0.08 (1/day)	Estimated
Θ	0.15 (1/day)	Estimated
λ	0.5 (1/day)	Estimated

4.1.3 Invariant Region

Let Ω be biological feasibility of the malaria transmission model described by Equations (3.1–3.9) which requires that the solutions remain non-negative and bounded for all time $t \geq 0$. To guarantee that the model has epidemiological meaning, we establish the existence of a positively invariant region in which the model dynamics are biologically relevant. Let the sum of all human compartments at time t be denoted by equation (4.14)

$$N_H(t) = S_H(t) + E(t) + I_C(t) + I_F(t) + T_P(t) + T_n(t) + R(t), \tag{4.14}$$

From total mosquito population equation 4.11 which is given by

$$N_V(t) = S_V(t) + I_V(t).$$

Using the formulated system of equations (3.1–3.7), the variation in the total human population over time is expressed by:

$$\frac{dN_H}{dt} = \pi - \mu N_H(t).$$

Solving this first-order linear differential equation gives:

$$N_H(t) = N_H(0) - \left(\frac{\pi}{\mu}\right)^{(e^{-\mu t})} + \frac{\pi}{\mu}.$$

As $t \to \infty$, (4.15)

The exponential term vanishes, and the human population approaches the steady-state value:

$$N_H(t) \to \frac{\pi}{\mu}.$$

Hence, the total human population is bounded by $0 < N_H(t) \leq \frac{\pi}{\mu}$ for all $t \geq 0$. Similarly, for the mosquito population, summing Equations (3.8-3.9) gives:

$$\frac{dN_V}{dt} = \wedge - \mu N_V(t). \tag{4.16}$$

Solving equation 4.16 yields equation 4.17:

$$N_V(t) = N_V(0) - \left(\frac{\wedge}{\mu}\right)^{(e^{-\mu t})} + \frac{\wedge}{\mu}.$$

As $t \to \infty$, (4.17)

to obtain the limiting value:

$$N_V(t) \to \frac{\pi}{\mu}.$$

Therefore, $0 < N_V(t) \leq \frac{\triangle}{\mu}$ for all $t \geq 0$.

Thus, all the model solutions describing malaria transmission dynamics are contained in the compact invariant region:

$$\Omega = S_H(t) + E(t) + I_C(t) + I_F(t) + T_P(t) + T_n(t) + R(t) \in \mathbb{R}^9_+ : \tag{4.18}$$

$$N_H \leq \frac{\pi}{\mu}, \quad N_V \leq \frac{\wedge}{\mu}.$$

Hence, Ω is positively invariant and attracts all trajectories of the system. This implies that the model solutions are epidemiologically and mathematically meaningful within Ω.

4.1.4 Disease-Free Equilibrium Point

Assuming no individuals are infected humans or mosquitoes. Therefore, $I_C = I_F = T_P = T_n = I_V = 0$ (4.19)

Since there is no infection, exposed individuals $(E) = 0$. Solving for S_H, R and S_V, then equation (3.1) gives equation 4.20;

$$\frac{dS_H}{dt} = \pi - \alpha S_H - \mu S_H = 0 \tag{4.20}$$

Solving for S_H^* (DFE value of S_H) from equation 4.20 gives equation 4.21;

$$S_H^* = \frac{\pi}{\alpha + \mu} \tag{4.21}$$

From equation (3.7), where $T_P = T_n = 0$:

$$\frac{dR}{dt} = -\rho R - \mu R = 0 \tag{4.22}$$

Thus, $R^* = 0$.

From equation (3.8) which simplifies to

$$\frac{dS_V}{dt} = \wedge - \psi S_V - \mu S_V = 0 \tag{4.23}$$

Solving for S_V^*;

$$S_V^* = \frac{\wedge}{\psi + \mu}$$

Since $I_V = 0$, infection force $\lambda = 0$.

Thus, DFE is ;

$$(E^0 = S_H^0, E^0, I_C^0, I_F^0, T_P^0, T_n^0, R^0, S_V^0, I_V^0) = \left(\frac{\pi}{\alpha+\mu}, 0, 0, 0, 0, 0, 0, \frac{\wedge}{\psi+\mu}, 0\right) \tag{4.24}$$

Then the D.F.E point (E^0) which represents the infection; the equilibrium point corresponding to the absence of infection (3.1–3.9), is numerically in figure 4.1 below.

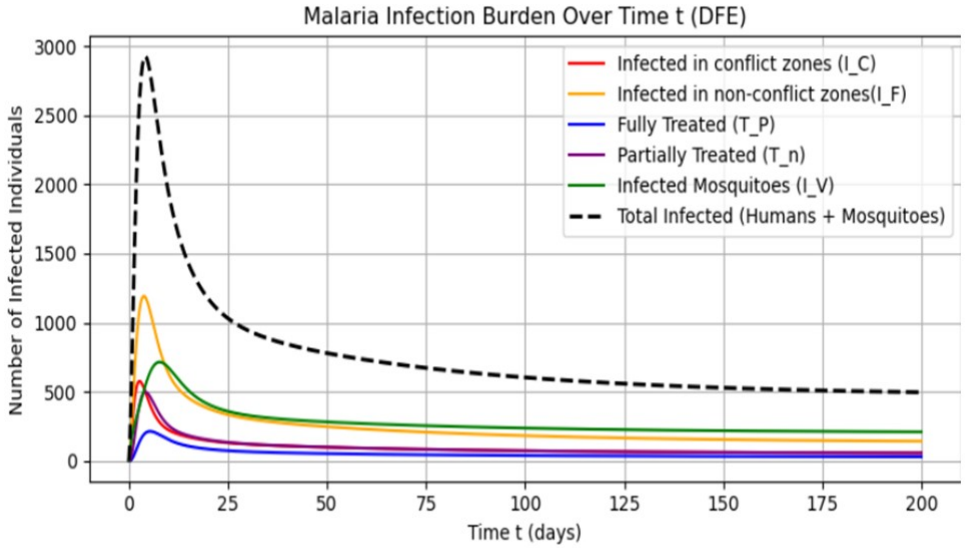

Figure 4.1: Malaria Infection Burden over Time

This figure1 depicts the dynamic behavior of malaria spread infection over time at the disease-free equilibrium (DFE). At the onset, infection levels in both conflict and non-conflict regions increase rapidly, representing a short-lived outbreak phase before gradually declining. As time progresses, the infected and treated human groups, along with the mosquito population, consistently decrease and stabilize around zero, demonstrating convergence to the DFE. The overall infection curve (shown by the black dashed line) drops swiftly and subsequently stabilizes, suggesting that malaria transmission has been effectively suppressed and the disease eventually disappears from the population.

4.1.5 Computation of Basic Reproduction Number

The next-generation matrix technique is applied to derive the basic reproduction number, R_0 with respect to the model, following the method outlined as proposed by van den Driessche and Watmough, (2002). If $R_0 > 1$, the infection is likely to propagate throughout the population, thereby causing an epidemic and therefore existence pertaining to a stable endemic equilibrium point (EEP). Conversely, if $R_0 < 1$, the infection eventually dies out, leading the system to approach a stable disease-free equilibrium (DFE).

In this method, f represent matrix of the new infections while v represent the remaining transition terms, such as recovery or progression between compartments, excluding new infections. From equation 3.3–3.7, let

$$\begin{aligned}
\frac{dI_C}{dt} &= \lambda E - \Omega_1 I_C, \quad \text{where } \Omega_1 = (\Phi + \Theta + 1 + \mu) \\
\frac{dI_f}{dt} &= (1-\lambda)E - \Omega_2 I_f, \quad \text{where } \Omega_2 = (v + e + \mu + \gamma) \\
\frac{dT_P}{dt} &= \omega I_C - \Omega_3 T_P, \quad \text{where } \Omega_3 = (\epsilon + \mu + x) \\
\frac{dT_n}{dt} &= (1-\omega) I_C - \Omega_4 T_n, \quad \text{where } \Omega_4 = (e + \mu + 1 - x) \\
\frac{dI_V}{dt} &= \psi S_v - \Omega_5 I_V, \quad \text{where } \Omega_5 = (z + \tau)
\end{aligned} \tag{4.25}$$

From system of equations (4.25) the vector of new infection terms going into compartment is given by equation (4.26);

$$f = \begin{bmatrix} \lambda E \\ (1-\lambda)E \\ 0 \\ 0 \\ 0 \end{bmatrix} \tag{4.26}$$

From equation (4.25), the transition vector of equation (4.27) yields;

$$v = \begin{bmatrix} +\Omega_1 I_C \\ +\Omega_2 I_f \\ -\omega I_C + \Omega_3 T_P \\ (\omega - 1) I_C + \Omega_4 T_n \\ -\psi S_V + \Omega_5 I_V \end{bmatrix} \tag{4.27}$$

The formulation of matrices F and V is achieved by computing the Jacobian derivative matrix of f and v from Mathematica software corresponding to the new infection of equation (4.26) terms and the transition terms in equation (4.27) respectively, obtained at the DFE

$$F = \begin{bmatrix} \beta E & \beta \hat{N}_1 E & \beta \hat{N}_2 E & \beta \hat{N}_3 E & \beta \hat{N}_4 E \\ (1-\beta) E & (1-\beta) E \hat{N}_1 & (1-\beta) E \hat{N}_2 & (1-\beta) \hat{N}_3 E & (1-\beta) \hat{N}_4 E \\ 0 & 0 & 0 & 0 & 0 \\ 0 & 0 & 0 & 0 & 0 \\ 0 & 0 & 0 & 0 & 0 \end{bmatrix} \tag{4.28}$$

Where I_C, I_V, I_f, T_n, and T_P are infected compartments.

$$V = \begin{bmatrix} \Omega_1 & 0 & 0 & 0 & 0 \\ 0 & 0 & \Omega_2 & 0 & 0 \\ -\omega & 0 & 0 & 0 & \Omega_3 \\ (\omega - 1) & 0 & 0 & \Omega_4 & 0 \\ 0 & \Omega_5 & 0 & 0 & 0 \end{bmatrix} \tag{4.29}$$

Finding inverse of Matrix of equation (4.29) yields equation (4.30);

$$V^{-1} = \begin{bmatrix} \frac{1}{\Omega_1} & 0 & 0 & 0 & 0 \\ 0 & 0 & \frac{1}{\Omega_2} & 0 & 0 \\ \frac{\omega}{\Omega_1\Omega_3} & 0 & \frac{1}{\Omega_3} & 0 & 0 \\ \frac{(1-\omega)}{\Omega_1\Omega_4} & 0 & 0 & \frac{1}{\Omega_4} & 0 \\ 0 & \frac{1}{\Omega_5} & 0 & 0 & 0 \end{bmatrix} \tag{4.30}$$

Computing FV^{-1}, this represents the next-generation matrix of equation (4.31);

$$FV^{-1} = \begin{bmatrix} \frac{\beta(-((-1+\omega)\hat{N}_3\Omega_3+(\omega\hat{N}_4+\Omega_3)\Omega_4))}{\Omega_1\Omega_3\Omega_4} & \frac{\beta\hat{N}_2}{\Omega_2} & \frac{\beta\hat{N}_4}{\Omega_3} & \frac{\beta\hat{N}_3}{\Omega_4} & \frac{\beta\hat{N}_1}{\Omega_5} \\ \frac{(-1+\beta)((-1+\omega)\hat{N}_3\Omega_3-(\omega\hat{N}_4+\Omega_3)\Omega_4)}{\Omega_1\Omega_3\Omega_4} & -\frac{(-1+\beta)\hat{N}_2}{\Omega_2} & -\frac{(-1+\omega)\hat{N}_4}{\Omega_3} & -\frac{(-1+\beta)\hat{N}_3}{\Omega_4} & -\frac{(-1+\beta)\hat{N}_1}{\Omega_5} \\ 0 & 0 & 0 & 0 & 0 \\ 0 & 0 & 0 & 0 & 0 \\ 0 & 0 & 0 & 0 & 0 \end{bmatrix} \tag{4.31}$$

Then, finding the Eigen values yields: $X_1 = 0$, $X_2 = 0$, $X_3 = 0$ and

$$X_4 = -\frac{(-\beta\hat{N}_3\Omega_2\Omega_3 + \beta\omega\hat{N}_3\Omega_2\Omega_3 - \beta\omega\hat{N}_4\Omega_2\Omega_4 - \hat{N}_2\Omega_1\Omega_3\Omega_4 + \beta\hat{N}_2\Omega_1\Omega_3\Omega_4 - \beta\Omega_2\Omega_3\Omega_4)}{\Omega_1\Omega_2\Omega_3\Omega_4} \tag{4.32}$$

Therefore,

$$R_0 = \frac{\Omega_1(\hat{N}_2 - \Omega_2)\Omega_3\Omega_4}{(-\hat{N}_3\Omega_2\Omega_3 + \omega\hat{N}_3\Omega_2\Omega_3 - \omega\hat{N}_4\Omega_2\Omega_4 + \hat{N}_4\Omega_1\Omega_3\Omega_3 - \Omega_2\Omega_3\Omega_4)} \tag{4.33}$$

This corresponds to the spectral radius, representing the dominant eigenvalue that governs the system's dynamics denoted by $[R_0]$. Generally, when $R_0 < 1$, each infection leads to less than one additional infection on average, leading to the eventual elimination of the disease, and thus the disease-free equilibrium becomes locally and globally asymptotically stable. Conversely, when $R_0 > 1$, an infected person contributes to

more than one additional infection in the population secondary infection on average, indicating that the disease will persist within the population.

4.1.6 Local Stability Analysis of DFE

Finding stability near the equilibrium point by constructing the Jacobian Matrix J based on nine malaria compartmental models. Implying, extracting and examining the portion of the Jacobian that controls the diseased compartments for the sake of conciseness, which are:

$$X = E, I_C, I_F, T_P, T_n, R, I_V$$

Evaluation of the Jacobian matrix J is evaluated at E_0. Determine the eigenvalues of this reduced Jacobian and then, the system is linearized around DFE. Apply the next-generation matrix approach, [Van den Driessche & Watmough, 2002].

Theorem 3 The disease-free equilibrium E_0 is locally asymptotically stable if $R_0 < 1$ and unstable if $R_0 > 1$. Then, calculate Jacobian matrix J for equation (3.1)–(3.9), such that

$$g_1 = \pi + I_V - \alpha S_H - \mu S_H$$

$$g_2 = \alpha S_H + \rho R - \lambda E - (1 - \lambda)E - \mu E$$

$$g_3 = \lambda E - \phi I_C - \Theta I_C - \omega I_C - (1 - \omega)I_C - \mu I_C$$

$$g_4 = (1 - \lambda)E - \nu I_F - \epsilon I_F - \mu I_F - \gamma I_F$$

$$g_5 = \omega I_C - \epsilon T_P - \mu T_P - X T_P$$

$$g_6 = (1-\omega)I_C - eT_n - \mu T_n - (1-x)T_n \tag{4.34}$$

$$g_7 = xT_P + \gamma I_F - \rho R - \mu R + (1-x)T_n$$

$$g_8 = \Lambda + \phi I_C + \nu I_F - \psi S_V - \mu S_V$$

$$g_9 = \psi S_V - zI_V - \tau I_V$$

The force of infection expressed by equation (3.10) as below:

$$\lambda = \frac{\beta(I_C + \hat{N}_1 I_V + \hat{N}_2 I_F + \hat{N}_3 T_n + \hat{N}_4 T_p)}{N}$$

The Jacobian matrix J associated with malaria framework is obtained and determined at DFE. Eigenvalues are analyzed to determine the condition for local stability of DFE.

Proof The Jacobian matrix framework is derived from equations (4.34) to equation (4.35)

$$J = \begin{bmatrix} -(\alpha+\mu)-\Psi & 0 & 0 & 0 & 0 & 0 & 0 & 0 & z \\ \alpha & -(1+\mu)-\Psi & 0 & 0 & 0 & 0 & \rho & 0 & 0 \\ 0 & 0 & (\beta-\phi-\theta-1-\mu)-\Psi & \beta\eta_2 & \beta\eta_4 & \beta\eta_3 & 0 & 0 & \beta\eta_1 \\ 0 & 1 & -\beta & -\beta\eta_2-\nu-\varepsilon-\mu-\gamma & -\beta\eta_4-\Psi & -\beta\eta_3 & 0 & 0 & -\beta\eta_1 \\ 0 & 0 & \omega & 0 & -(\varepsilon+\mu+\chi)-\Psi & 0 & 0 & 0 & 0 \\ 0 & 0 & 1-\omega & 0 & 0 & (-\varrho-\mu-1+\chi)-\Psi & 0 & 0 & 0 \\ 0 & 0 & 0 & 0 & \chi+\gamma & 1-\chi & -(\rho+\mu)-\Psi & 0 & 0 \\ 0 & 0 & \phi & 0 & \nu & 0 & 0 & -(\varphi+\mu)-\Psi & 0 \\ 0 & 0 & 0 & 0 & 0 & 0 & 0 & \varphi & -(\tau+z)-\Psi \end{bmatrix}$$

A Jacobian matrix's characteristic polynomial can be obtained by calculating the determinant of $|J - \lambda_i I| = 0$, where J is Jacobian Matrix with $i = 1, 2, 3, 4, 5, 6, 7, 8, 9$ and a Jacobian matrix's characteristic polynomial and λ is a scalar variable. According to Khalil (2002), the eigenvalues that establish system stability close to an equilibrium point are the roots of this polynomial.

Then, apply the Routh–Hurwitz criterion to determine whether those coefficients from equation (4.35) lead to all negative real parts of eigenvalues of equation (4.36).

$$X(\lambda) = \lambda^9 + \lambda^8 a_1 + \lambda^7 a_2 + \lambda^6 a_3 + \lambda^5 a_4 + \lambda^4 a_5 + \lambda^3 a_6 + \lambda^2 a_7 + \lambda^1 a_8 + a_9 \quad (4.36)$$

The conditions for all coefficients are:

$$a_1 > 0,\ a_2 > 0,\ a_3 > 0, \ldots, a_9 > 0 \quad (4.37)$$

The numerical values of coefficients of equation (4.37) represented in terms of $R_0^{(*)}$ as given by equation (4.38);

$$a_1 = 0, \quad a_2 = -\gamma - \epsilon - \mu - \nu - \beta\eta_2$$

$$\begin{aligned} a_3 = & -\beta^2\eta_2 - \beta\omega\eta_2 \\ & -(-1-\mu)(-\gamma-\epsilon-\mu-\nu-\beta\eta_2) \\ & +(\alpha+\mathcal{Z}+\mu+\tau)(-\gamma-\epsilon-\mu-\nu-\beta\eta_2) \\ & -(-1+\beta-\theta-\mu-\phi)(-\gamma-\epsilon-\mu-\nu-\beta\eta_2) \\ & -(-1-\mu-\varrho+)(-\gamma-\epsilon-\mu-\nu-\beta\eta_2) \\ & +(-\mu-\rho)(\gamma+\epsilon+\mu+\nu+\beta\eta_2) \\ & +(-\mu-\phi)(\gamma+\epsilon+\mu+\nu+\beta\eta_2) \\ & +(-\epsilon-\mu-\chi)(\gamma+\epsilon+\mu+\nu+\beta\eta_2) \end{aligned} \quad (4.38)$$

The appendix will include detailed coefficients a_4, a_5, a_6, a_7, a_8, and a_9 that are left out of the local stability analysis for simplicity.

4.1.7 Global Stability of Disease-Free Equilibrium (D.F.E)

The system of equations (3.1-3.9) can also be proved to lie in the positive region using theorem (4.1.6.1). The global stability of the disease-free equilibrium is evaluated through Marzler matrix stability approach proposed in the work of (catillo-chevez et al.2002)

$$\frac{dX}{dt} = F(X, Z), \qquad \frac{dZ}{dt} = G(X, Z),\ G(X, 0) \tag{4.39}$$

Where $X = (S_H, S_V, E, R) \in \mathbb{R}^4_+$

Represents the non-infectious malaria compartments and $Z = (I_C, T_P, T_n, I_F, I_V) \in \mathbb{R}^5_+$

Represent the infectious malaria compartment. $E_0 = (X^*, 0)$,

Corresponds to the disease-free equilibrium of the system when the following condition holds:

$$i.\frac{dX}{dt} = F(X, 0), \quad \text{such that } X^* \text{ is globally asymptotically stable}$$

ii.$\frac{dZ}{dt} = D_z G(X, 0)Z - G(X, Z) \geq 0$ for all $(X, Z) \in \Omega$,

Therefore, we conclude that the disease-free equilibrium E_0 is locally asymptotically stable, provided the following theorem is satisfied.

Theorem 4:

The equilibrium point $E_0(X^*, 0)$ of the system is globally asymptotically stable if $R_0^* \leq 1$ and the conditions (i) and (ii) are satisfied, otherwise unstable.

Proof:

Let $X = (S_H, S_V, E, R)$ and $Z = (I_C, T_P, T_n, I_F, I_V)$, (4.41)

The equation 4.40 is new variables and the sub-systems of the system model. From equation 4.40 the vector function $G(X, Z)$ are obtained, the reduced system is given by equation 4.41,

$$F(X,0) = \begin{pmatrix} \pi - \mu S_H \\ \wedge - \mu S_V \\ 0 \\ 0 \end{pmatrix} \tag{4.42}$$

It is noted that this is an asymptotic dynamics systems independent with respect to the initial conditions in equation 4.40 thus; the solutions of the reduced system (4.42) are globally convergent in equation 4.40, as shown by computing equation 4.43.

$$G^{\wedge}(X,Z) = D_z G(X^*,0)Z - G(X,Z)$$

$$G^{\wedge}(X,Z) \geq 0. \tag{4.43}$$

Now, let A denote equation 4.44

$$A = D_z G(X^*, 0), \tag{4.44}$$

Which represent the Jacobian of $G^{\wedge}(X, Z)$ determined at $(I_C, T_P, T_n, I_F, I_V)$ and evaluated at $(x^*, 0)$, with the matrix A expressed as equation 4.45;

$$A = \begin{pmatrix} \Omega_1 & \beta\hat{N}_2 & \beta\hat{N}_4 & \beta\hat{N}_3 & \beta\hat{N}_1 \\ -\beta & -\beta\hat{N}_2 - \Omega_2 & -\beta\hat{N}_4 & -\beta\hat{N}_3 & -\beta\hat{N}_1 \\ \omega & 0 & \Omega_3 & 0 & 0 \\ 1-\omega & 0 & 0 & \Omega_4 & 0 \\ \Phi & 0 & \vee & 0 & 0 \end{pmatrix} \tag{4.45}$$

Where

$$\beta - \Phi - \Theta - 1 - \mu = \Omega_1$$

$$- \vee -\epsilon - \mu - \gamma = \Omega_2$$

$$-\epsilon - \mu - x = \Omega_3$$

$$-e - \mu - 1 + x = \Omega_4$$

The function $G^{\wedge}(X, Z)$ is expressed in matrix form as equation 4.46

$$AZ = \begin{pmatrix} (1 - S/N)\beta(I_C + \hat{N}_1 I_V + \hat{N}_2 I_F + \hat{N}_3 T_n + \hat{N}_4 T_p) \\ 0 \\ 0 \\ 0 \\ 0 \end{pmatrix} \tag{4.46}$$

Therefore, if the condition $G(X, Z) \geq 0$, the disease-free equilibrium (E_0) is globally asymptotically stable if the condition holds; otherwise, it is unstable. Since $G(X, Z)$, $S_H \leq N$, $S_H/N \leq 1$, then $G(X, Z) \geq 0 \forall\, X, Z \in \mathbb{R}^5_+$, hence, the disease-free equilibrium is globally asymptotically stable. Moreover, the matrix of equation 4.45 is an AZ-matrix of equation 4.46 by virtue of having non-negative off-diagonal entries. This proves global disease-free equilibrium (G.D.F.E) is global asymptotically stability of the disease-free equilibrium. Hence prove. This demonstrates that Malaria dies out whenever $R_0^* < 1$, irrespective of the initial conditions.

4.1.8 Existence of Endemic Equilibrium Point (E.E.P)

Theorem 5: The Endemic Equilibrium Point (EEP) exists whenever $R_0 > 1$.

Proof: The existence of the endemic equilibrium requires that all infectious compartments take strictly positive equilibrium values, $I_C > 0,\ I_F > 0,\ T_P > 0,\ T_n > 0$ and $I_V > 0$.

Where,

$$I_C = \lambda E - (\Phi + \Theta + \omega - (1 - \omega) + \mu) I_C. \tag{4.47}$$

This implies that

$$A = \Phi + \Theta + 1 + \mu, \quad \text{Therefore}$$

$$I_C = \frac{\lambda E}{A}. \tag{4.48}$$

Also,

$$I_F = (1 - \lambda)E - (v + e + \mu + \gamma)I_F.$$

Let $B = v + e + \mu + \gamma$,

Therefore

$$I_F = \frac{(1 - \lambda)E}{B}. \tag{4.49}$$

Also,

$$T_P = \omega I_C - (\epsilon + \mu + X)T_P,$$

Let $C = \epsilon + \mu + X$,

Therefore,

$$T_P = \frac{\omega I_C}{C}. \tag{4.50}$$

Also,

$$T_n = (1 - \omega)I_C - (\epsilon + \mu + (1 - X))T_n.$$

Let $D = \epsilon + \mu + (1 - X)$,

Therefore,

$$T_n = \frac{(1 - \omega)I_C}{D}. \tag{4.51}$$

Also,

$$I_V = \psi S_V - (z + \tau)I_V,$$

Let $G = z + \tau$,

Therefore,

$$I_V = \frac{\psi S_V}{G}. \tag{4.52}$$

Substituting equations (4.48–4.52) into equation (3.10) yields equation (4.53),

$$\lambda = \frac{\beta}{N}\beta\left[\frac{\lambda E}{A} + \hat{\eta}_1\frac{\psi S_V}{G} + \hat{\eta}_2\frac{(1-\lambda)E}{B} + \hat{\eta}_3\frac{(1-\omega)\lambda\lambda E/A}{D} + \hat{\eta}_4\frac{\lambda E}{AC}\right]. \quad (4.53)$$

Group terms:

$$\lambda = \frac{\beta}{N}\left[\frac{\lambda E}{A} + \hat{\eta}_1\frac{\psi S_V}{G} + \hat{\eta}_2\frac{(1-\lambda)E}{B} + \frac{\lambda E}{A}\left(\frac{\hat{\eta}_3(1-\omega)}{D} + \frac{\hat{\eta}_4\omega}{C}\right)\right],$$

Group λE terms:

$$\lambda = \frac{\beta}{N}\left[\hat{\eta}_1\frac{\psi S_V}{G} + \frac{(1-\lambda)E\hat{\eta}_2}{B} + \frac{\lambda E}{A}\left(1 + \frac{\hat{\eta}_3(1-\omega)}{D} + \frac{\hat{\eta}_4\omega}{C}\right)\right].$$

Let

$$M = \frac{1}{A}\left(1 + \frac{\hat{\eta}_3(1-\omega)}{D} + \frac{\hat{\eta}_4\omega}{C}\right), \quad F = \hat{\eta}_1\frac{\psi S_V}{G}, \quad Q = \frac{\hat{\eta}_2 E}{B}.$$

Solving for λ yields

$$\lambda = \frac{(\beta F + Q)}{(N + \beta Q - \beta E M)} > 1. \quad (4.54)$$

Hence, E.E.P proved.

Therefore, a numerical illustration of the endemic equilibrium point is presented in the figure 4.2.

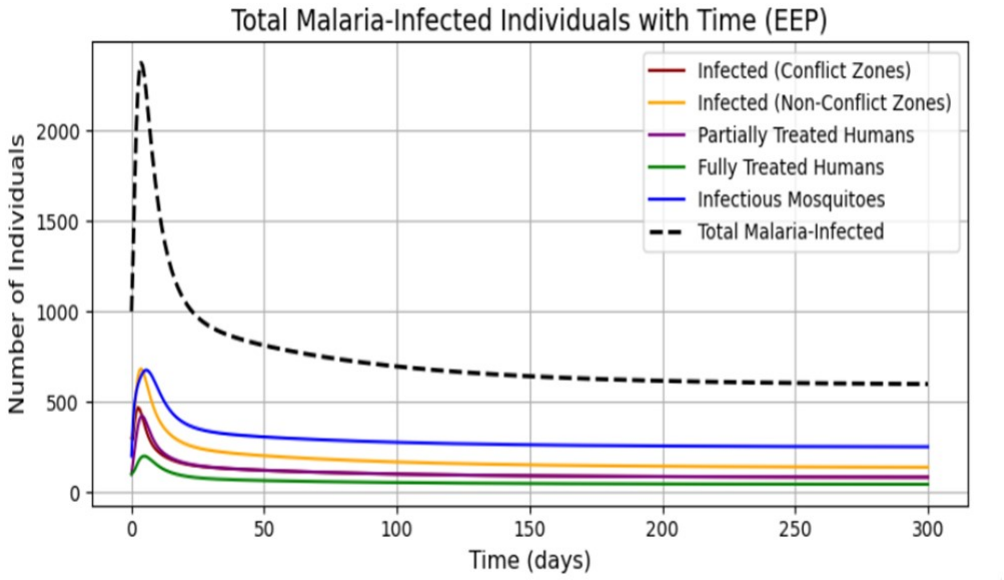

Figure 4.2: Total Malaria People who are infected over Time

Figure 4.2 illustrates the advancement of malaria transmission infection dynamics over time, converging toward the endemic equilibrium point (EEP). Initially, the prevalence of infection within the population and infectious mosquitoes rises sharply before gradually declining and stabilizing at a constant level. This stabilization signifies that the disease persists in the population at a steady state rather than being eradicated. The higher infection levels in conflict zones compared to non-conflict zones indicate that instability and limited healthcare access contribute to sustained transmission.

4.1.9 Global Stability Analysis of the Endemic Equilibrium point

A Lyapunov function criterion is applied to establish conditions required for the stability of the endemic equilibrium point. This involved identifying necessary conditions of the derivative of the Lyapunov function to be negative definite, which confirms global asymptotic stability for reduced equations (3.1–3.9); then simplifying the system by introducing Ω_i yields equation (4.55):

$$
\begin{aligned}
\frac{dS_H}{dt} &= \pi + \mathbb{Z}I_V - \alpha S_H - \mu S_H = \pi + \mathbb{Z}I_V - \Omega_1 S_H, \\
\frac{dE}{dt} &= \alpha S_H + \rho R - \lambda E - (1-\lambda)E - \mu E = \alpha S_H + \rho R - \Omega_2 E, \\
\frac{dI_C}{dt} &= \lambda E - \phi I_C - \Theta I_C - \omega I_C - (1-\omega)I_C - \mu I_C = \lambda E - \Omega_3 I_C, \\
\frac{dI_F}{dt} &= (1-\lambda)E - vI_F - \epsilon I_F - \mu I_F - \gamma I_F = (1-\lambda)E - \Omega_4 I_F, \\
\frac{dT_P}{dt} &= \omega I_C - \epsilon T_P - \mu T_P - XT_P = \omega I_C - \Omega_5 T_P, \\
\frac{dT_n}{dt} &= (1-\omega)I_C - eT_n - \mu T_n - (1-x)T_n = (1-\omega)I_C - \Omega_6 T_n, \\
\frac{dR}{dt} &= xT_P + \gamma I_F - \rho R - \mu R + (1-x)T_n = xT_P + (1-x)T_n + \gamma I_F - \Omega_7 R, \\
\frac{dS_V}{dt} &= \Lambda + \phi I_C + vI_F - \psi S_V - \mu S_V = \Lambda + \phi I_C + vI_F - \Omega_8 S_V, \\
\frac{dI_V}{dt} &= \psi S_V - zI_V - \tau I_V = \psi S_V - \Omega_9 I_V.
\end{aligned} \tag{4.55}
$$

Therefore, the control reproduction number (R_0^*), the force of infection (λ^*), and the D.F.E are given by equation (4.56).

$$
E^0 = (S_H^0, E^0, I_C^0, I_F^0, T_P^0, T_n^0, R^0, S_V^0, I_V^0) = \left(\frac{\pi}{\mu}, 0, 0, 0, 0, 0, 0, 0, 0, 0\right) \tag{4.56}
$$

and $E.E.P$

$$
E^* = (S^*, E^*, I_C^*, I_F^*, T_P^*, T_n^*, R^*, S_V^*, I_V^*).
$$

The system of R_0^* is given by equation (4.57):

$$
R_0^* = \frac{\beta}{N}\left(\frac{S^0}{\Omega_1} + \frac{S^0\hat{\eta}_1}{\Omega_1\Omega_6} + \frac{S^0\hat{\eta}_2}{\Omega_1\Omega_2} + \frac{S^0\hat{\eta}_3}{\Omega_1\Omega_4} + \frac{S^0\hat{\eta}_4}{\Omega_1\Omega_3}\right) \tag{4.57}
$$

The system of equation in (4.55) from Lyapunov function is given by equation (4.58)

$$K(S_H, E, I_C, I_F, T_P, T_n, R, S_V, I_V) = S_H - S_H^* - S_H^* \ln \frac{S_H}{S_H^*} + y_1(E - E^* - E^* \ln \frac{E}{E^*}) + y_2(I_C - I_C^* - I_C^* \ln \frac{I_C}{I_C^*}) + y_3(I_F - I_F^* - I_F^* \ln \frac{I_F}{I_F^*}) + y_4(T_P - T_P^* - T_P^* \ln \frac{T_P}{T_P^*}) + y_5(T_n - T_n^* - T_n^* \ln \frac{T_n}{T_n^*}) + y_6(R - R^* - R^* \ln \frac{R}{R^*}) + y_7(S_V - S_V^* - S_V^* \ln \frac{S_V}{S_V^*}) + y_8(I_V - I_V^* - I_V^* \ln \frac{I_V}{I_V^*}). \tag{4.58}$$

$y_1, y_2, \ldots, y_8$ are all positive to be determined as follows.

The Lyapunov function for the system is constructed as follows $K(S_H, E, I_C, I_F, T_P, T_n, R, S_V, I_V)$ that satisfies the condition

$$K(S^*, E^*, I_C^*, I_F^*, T_P^*, T_n^*, R^*, S_V^*, I_V^*) = 0$$

and

$$K(S_H, E, I_C, I_F, T_P, T_n, R, S_V, I_V) > 0,$$

hence it's definite as in equation (4.59):

$$\frac{dK(S_H, E, I_C, I_F, T_P, T_n, R, S_V, I_V)}{dt}. \tag{4.59}$$

For it to be negative definite, it must satisfy equations (4.60) and (4.61),

$$\frac{dK(S_H^*, E^*, I_C^*, I_F^*, T_P^*, T_n^*, R^*, S_V^*, I_V^*)}{dt} = 0, \tag{4.60}$$

and

$$\frac{dK(S_H^*, E^*, I_C^*, I_F^*, T_P^*, T_n^*, R^*, S_V^*, I_V^*)}{dt} < 0. \tag{4.61}$$

Therefore, the $E.E.P$

$$E^* = (S^*, E^*, I_C^*, I_F^*, T_P^*, T_n^*, R^*, S_V^*, I_V^*)$$

for the system that satisfies equation (4.62),

$$\begin{aligned}
\pi &= \alpha S_H^{**} + \mu S_H^{**} - \mathbb{Z} I_V^{**}, \\
\Omega_2^{**} E^{**} &= \alpha^{**} S_H^{**} + \rho^{**} R^{**}, \\
\Omega_3^{**} I_C^{**} &= \lambda^{**} E^{**}, \\
(1-\lambda)^{**} E^{**} &= \Omega_4 I_F^{**}, \\
\omega I_C^{**} &= \Omega_5 T_P^{**}, \\
(1-\omega) I_C^{**} &= \Omega_6 T_n^{**}, \\
x T_P^{**} + (1-x) T_n^{**} + \gamma I_F^{**} &= \Omega_7 R^{**}, \\
\Lambda + \phi I_C^{**} + \upsilon I_F^{**} &= \Omega_8 S_V^{**}, \\
\psi S_V^{**} &= \Omega_9 I_V^{**}.
\end{aligned} \tag{4.62}$$

Simplifying and evaluating the Lyapunov derivatives gives equation (4.63):

$$\begin{aligned}
\frac{dK(S_H, E, I_C, I_F, T_P, T_n, R, S_V, I_V)}{dt} &= (1 - \frac{S_H^{**}}{S_H})\frac{dS_H}{dt} + y_1(1 - \frac{E^{**}}{E})\frac{dE}{dt} + y_2(1 - \frac{I_C^{**}}{I_C})\frac{dI_C}{dt} \\
&+ y_3(1 - \frac{I_F^{**}}{I_F})\frac{dI_F}{dt} + y_4(1 - \frac{T_P^{**}}{T_P})\frac{dT_P}{dt} + y_5(1 - \frac{T_n^{**}}{T_n})\frac{dT_n}{dt} \\
&+ y_6(1 - \frac{R^{**}}{R})\frac{dR}{dt} + y_7(1 - \frac{S_V^{**}}{S_V})\frac{dS_V}{dt} + y_8(1 - \frac{I_V^{**}}{I_V})\frac{dI_V}{dt}.
\end{aligned} \tag{4.63}$$

Substituting $\frac{dS_H}{dt}, \frac{dE}{dt}, \frac{dI_C}{dt}, \frac{dI_F}{dt}, \frac{dT_P}{dt}, \frac{dT_n}{dt}, \frac{dR}{dt}, \frac{dS_V}{dt}, \frac{dI_V}{dt}$ in equation (4.63) yields equation (4.64)

$$\frac{dK(S_H, E, I_C, I_F, T_P, T_n, R, S_V, I_V)}{dt} = \left(1 - \frac{S_H^{**}}{S_H}\right)(\alpha S_H^{**} + \mu S_H^{**} - \mathbb{Z} I_V^{**} + \mathbb{Z} I_V - \Omega_1 S_H)$$
$$+ y_1 \left(1 - \frac{E^{**}}{E}\right)(\alpha S_H + \rho R - \Omega_2 E)$$
$$+ y_2 \left(1 - \frac{I_C^{**}}{I_C}\right)(\lambda E - \Omega_3 I_C)$$
$$+ y_3 \left(1 - \frac{I_F^{**}}{I_F}\right)\big((1-\lambda)E - \Omega_4 I_F\big)$$
$$+ y_4 \left(1 - \frac{T_P^{**}}{T_P}\right)(\omega I_C - \Omega_5 T_P)$$
$$+ y_5 \left(1 - \frac{T_n^{**}}{T_n}\right)\big((1-\omega) I_C - \Omega_6 T_n\big)$$
$$+ y_6 \left(1 - \frac{R^{**}}{R}\right)\big(x T_P + (1-x) T_n + \gamma I_F - \Omega_7 R\big)$$
$$+ y_7 \left(1 - \frac{S_V^{**}}{S_V}\right)(\Lambda + \phi I_C + v I_F - \Omega_8 S_V)$$
$$+ y_8 \left(1 - \frac{I_V^{**}}{I_V}\right)(\psi S_V - \Omega_9 I_V). \tag{4.64}$$

$$
\begin{aligned}
P = & \left[\left(\frac{\beta\big(\hat{N}_1 I_V(t) + \hat{N}_2 I_F(t) + \hat{N}_3 T_n(t) + \hat{N}_4 T_P(t) + I_C\big)}{E(t) + I_C(t) + I_F(t) + R(t) + S_H(t) + T_P(t) + T_n(t)} - 1\right) E(t)\right] \\
& + \left(\frac{I_C^{(**)}}{I_C(t)} - 1\right)\left[-\left(\frac{\beta\big(\hat{N}_1 I_V(t) + \hat{N}_2 I_F(t) + \hat{N}_3 T_n(t) + \hat{N}_4 T_P(t) + I_C\big)}{E(t) + I_C(t) + I_F(t) + R(t) + S_H(t) + T_P(t) + T_n(t)}\right.\right. \\
& \left.\left. + \mu I_C(t) + \omega I_C(t) + \phi I_C(t) + \theta I_C(t) - (\omega - 1) I_C(t)\right)\right] \\
& + \left(\frac{I_F^{(**)}}{I_F(t)} - 1\right)\left[\epsilon I_F(t) + \gamma I_F(t) + \mu I_F(t) + \nu I_F(t)\right. \\
& \left. + \left(\frac{\beta\big(\hat{N}_1 I_V(t) + \hat{N}_2 I_F(t) + \hat{N}_3 T_n(t) + \hat{N}_4 T_P(t) + I_C\big)}{E(t) + I_C(t) + I_F(t) + R(t) + S_H(t) + T_P(t) + T_n(t)} - 1\right) E(t)\right] \\
& + \left(\frac{I_V^{(**)}}{I_V(t)} - 1\right)\big(-\psi S_V(t) + \tau I_V(t) + z I_V(t)\big) \\
& + \left(\frac{R^{(**)}}{R(t)} - 1\right)\big(-\gamma I_F(t) + \mu R(t) + \rho R(t) - x T_P(t) + (x-1) T_n(t)\big) \\
& + \left(\frac{S_H^{(**)}}{S_H(t)} - 1\right)\big(\alpha S_H(t) + \mu S_H(t) - \pi - z I_V(t)\big) \\
& + \left(\frac{T_P^{(**)}}{T_P(t)} - 1\right)\big(X T_P(t) + \epsilon T_P(t) + \mu T_P(t) - \omega I_C(t)\big) \\
& + \left(\frac{T_n^{(**)}}{T_n(t)} - 1\right)\big(e T_n(t) + \mu T_n(t) + (\omega - 1) I_C(t) - (x-1) T_n(t)\big)
\end{aligned}
\tag{4.65}
$$

$$
\begin{aligned}
Q = & -\left(\frac{E^{(**)}}{E(t)} - 1\right)\left[\alpha S_H(t) - \frac{\beta\, E(t)\left(\hat{N}_1 I_V(t) + \hat{N}_2 I_F(t) + \hat{N}_3 T_n(t) + \hat{N}_4 T_P(t) + I_C(t)\right)}{E(t) + I_C(t) + I_F(t) + R(t) + S_H(t) + T_P(t) + T_n(t)}\right. \\
& - \mu E(t) + \rho R(t) \\
& \left. - \left(\frac{S_V^{(**)}}{S_V(t)} - 1\right)\big(\Lambda - \mu S_V(t) + \phi I_C(t) - \psi S_V(t) + \nu I_F(t)\big)\right]
\end{aligned}
$$

Where $\frac{dK}{dt} = 0$ holds only when $(S_H = S_H^{**}, E = E^{**}, I_C = I_C^{**}, I_F = I_F^{**}, T_P = T_P^{**}, T_n = T_n^{**}, R = R^{**}, S_V = S_V^{**}, I_V = I_V^{**})$, then the maximal compact invariant set in which $(S, E, I) \in \cap : \frac{dv}{dt} = 0$ is a singleton set, namely E_*^{**}.

By Lasalle's invariance principle, $\frac{dL(S,I,A,R)}{dt} < 0$ if and only if $P > Q$ (Mukandavire et al., 2010). The outcome indicates malaria will continue to exist whenever $P > Q$, regardless of the initial conditions.

4.1.10 Bifurcation Analysis

This approach will be used to investigate the presence of both backward and forward bifurcations.

Theorem: The framework exhibits a forward bifurcation at $R_0 = 1$. Hence, the endemic equilibrium point E^* is locally asymptotically stable for $R_0 > 1$ but close to 1.
Proof: Perform a bifurcation analysis using the Centre Manifold Theorem **?**. Rewrite the human compartment of the system using notations for simplicity. Let

$$y_1 = S_H,\ y_2 = E,\ y_3 = I_C,\ y_4 = I_F,\ y_5 = T_n,\ y_6 = T_P,\ y_7 = R,\ y_8 = S_V,\ y_9 = I_V,$$

hence

$$N = y_1 + y_2 + y_3 + y_4 + y_5 + y_6 + y_7 + y_8 + y_9 \tag{4.67}$$

Let

$$y = (y_1, y_2, y_3, y_4, y_5, y_6, y_7, y_8, y_9)^T \tag{4.68}$$

The framework (3.1–3.9) is written as

$$\frac{dy}{dt} = F(y) \tag{4.69}$$

with

$$F = (f_1, f_2, f_3, f_4, f_5, f_6, f_7, f_8, f_9)^T \tag{4.70}$$

where

$$\begin{aligned}
\frac{dS_H}{dt} &= f_1 = \pi + \Lambda I_V - y_1 S_H, \\
\frac{dE}{dt} &= f_2 = \alpha S_H + \rho R - y_2 E, \\
\frac{dI_C}{dt} &= f_3 = \lambda E - y_3 I_C, \\
\frac{dI_F}{dt} &= f_4 = (1-\lambda) E - y_4 I_F, \\
\frac{dT_P}{dt} &= f_5 = \omega I_C - y_5 T_P, \\
\frac{dT_n}{dt} &= f_6 = (1-\omega) I_C - y_6 T_n, \\
\frac{dR}{dt} &= f_7 = x T_P + (1-x) T_n + \gamma I_F - y_7 R, \\
\frac{dS_V}{dt} &= f_8 = \Lambda + \phi I_C + \nu I_F - y_8 S_V, \\
\frac{dI_V}{dt} &= f_9 = \psi S_V - y_9 I_V,
\end{aligned}$$

and

$$\lambda = \beta^* \frac{I_C + \beta_1 I_V + \beta_2 I_F + \beta_3 T_n + \beta_4 T_P}{N}.$$

The Jacobian of system (4.70) at the disease-free equilibrium is

$$J(E^0, \beta^*) = \begin{pmatrix}
-\Omega_1 & 0 & 0 & 0 & 0 & 0 & 0 & 0 & \zeta \\
\alpha & \Omega_2 & 0 & 0 & 0 & 0 & \rho & 0 & 0 \\
0 & 0 & -\Omega_3 & 0 & 0 & 0 & 0 & 0 & 0 \\
0 & 1 & 0 & -\Omega_4 & 0 & 0 & 0 & 0 & 0 \\
0 & 0 & \omega & 0 & -\Omega_5 & 0 & 0 & 0 & 0 \\
0 & 0 & 1-\omega & 0 & 0 & -\Omega_6 & 0 & 0 & 0 \\
0 & 0 & 0 & \gamma & x & 1-x & -\Omega_7 & 0 & 0 \\
0 & 0 & \phi & v & 0 & 0 & 0 & -\Omega_8 & 0 \\
0 & 0 & 0 & 0 & 0 & 0 & 0 & \psi & -\Omega_9
\end{pmatrix} \tag{4.71}$$

Considering the case $R_0 = 1$ and letting $\beta = \beta^*$ as a bifurcation parameter, solving β from $R_0 = 1$ gives

$$\beta = \beta^* = \frac{\mu N}{\pi} \left[\frac{\omega}{\Omega_3 \Omega_5} + \frac{1-\omega}{\Omega_3 \Omega_6} + \frac{\gamma}{\Omega_4} + \frac{\eta_2}{\Omega_4} + \frac{\eta_3}{\Omega_6} + \frac{\eta_4}{\Omega_5} + \frac{\Lambda \psi \eta_1}{\mu \Omega_9} \right]^{-1} \tag{4.72}$$

At $\beta = \beta^*$, $J(E^*)$ has a simple zero eigenvalue. Applying Center Manifold Theory, $J(E^*)$ near β^* has right and left eigenvectors corresponding to the zero eigenvalue:

$$k = (k_1, k_2, k_3, k_4, k_5, k_6, k_7, k_8, k_9)^T, \quad l = (l_1, l_2, l_3, l_4, l_5, l_6, l_7, l_8, l_9)^T.$$

Multiplying the right eigenvector k with $J(E^0, \beta^*)$ and equating to zero gives

$$k_1 = 1, \quad k_2 = \frac{1}{\Omega_4}, \quad k_3 = \frac{1}{\Omega_2\Omega_4}, \quad k_4 = \frac{1-\omega}{\Omega_3\Omega_6},$$
$$k_5 = \frac{\omega}{\Omega_3\Omega_5}, \quad k_6 = \frac{\gamma}{\Omega_1\Omega_7} + \frac{1-x}{\Omega_6\Omega_7} + \frac{x}{\Omega_5\Omega_7}, \quad k_7 = \frac{\phi}{\Omega_3\Omega_9} + \frac{v}{\Omega_4\Omega_9}.$$

Similarly, for the left eigenvector l:

$$l_1 = 1, \quad l_2 = \frac{1}{\Omega_2}, \quad l_3 = \frac{1}{\Omega_2\Omega_4}, \quad l_4 = \frac{1-x}{\Omega_6\Omega_7}, \quad l_5 = \frac{x}{\Omega_5\Omega_7}, \quad l_6 = \frac{\rho}{\Omega_2\Omega_7}, \quad l_7 = \frac{\phi}{\Omega_3\Omega_9} + \frac{v}{\Omega_4\Omega_9}.$$

The transpose of the Jacobian is

$$J(E^0, \beta^*)^T = \begin{pmatrix} -\Omega_2 & 0 & 1 & 0 & 0 & 0 & 0 \\ 0 & -\Omega_3 & 0 & 1-\omega & \omega & 0 & \phi \\ 0 & 0 & -\Omega_4 & 0 & 0 & \gamma & v \\ 0 & 0 & 0 & -\Omega_6 & 0 & 1-x & 0 \\ 0 & 0 & 0 & 0 & -\Omega_5 & x & 0 \\ \rho & 0 & 0 & 0 & 0 & -\Omega_7 & 0 \\ 0 & 0 & 0 & 0 & 0 & 0 & -\Omega_9 \end{pmatrix} \tag{4.73}$$

Multiply l with $J(E^0, \beta^*)^T$ and equate to zero to obtain the same left eigenvector above, satisfying the condition for applying Center Manifold Theory near $R_0 = 1$ with $\beta = \beta^*$.

Now compute the bifurcation coefficients a and b. Since $l_1 = 0$, compute the partial derivatives of $f_1, f_2, \ldots, f_9$ at the disease-free equilibrium. The nonzero second-order partial derivatives are:

For $f_3 = \lambda E - \Omega_3 I_C$:

$$\frac{\partial^2 f_3}{\partial I_C \partial E} = \frac{\beta}{N}, \quad \frac{\partial^2 f_3}{\partial I_V \partial E} = \frac{\beta\eta_1}{N}, \quad \frac{\partial^2 f_3}{\partial I_F \partial E} = \frac{\beta\eta_2}{N}, \quad \frac{\partial^2 f_3}{\partial T_n \partial E} = \frac{\beta\eta_3}{N}, \quad \frac{\partial^2 f_3}{\partial T_P \partial E} = \frac{\beta\eta_4}{N} \tag{4.74}$$

For $f_4 = (1-\lambda)E - \Omega_4 I_F$:

$$\frac{\partial^2 f_4}{\partial I_C \partial E} = -\frac{\beta}{N}, \quad \frac{\partial^2 f_4}{\partial I_V \partial E} = -\frac{\beta\eta_1}{N}, \quad \frac{\partial^2 f_4}{\partial I_F \partial E} = -\frac{\beta\eta_2}{N}, \quad \frac{\partial^2 f_4}{\partial T_n \partial E} = -\frac{\beta\eta_3}{N}, \quad \frac{\partial^2 f_4}{\partial T_P \partial E} = -\frac{\beta\eta_4}{N} \tag{4.75}$$

The bifurcation coefficients a and b are computed as

$$a = \frac{\beta k_2}{N}(l_3 - l_4)(k_3 + \eta_1 k_9 + \eta_2 k_4 + \eta_3 k_5 + \eta_4 k_6) \tag{4.76}$$

$$b = \frac{k_2}{N}(l_3 - l_4)(k_3 + \eta_1 k_9 + \eta_2 k_4 + \eta_3 k_5 + \eta_4 k_6) \tag{4.77}$$

If $a < 0$ and $b > 0$, the model exhibits a forward bifurcation, where the disease-free equilibrium is locally asymptotically stable when $R_0 < 1$, and a unique endemic equilibrium exists and is stable when $R_0 > 1$.

If $a > 0$ and $b > 0$, the model exhibits a backward bifurcation, indicating the possibility of multiple endemic equilibria coexisting with the disease-free state when $R_0 < 1$, and thus, control strategies must lower R_0 significantly below 1 to eliminate the disease. Hence proved.

4.1.11 Normalizing Sensitivity Analysis of Basic Reproduction Number

Sensitivity analysis which is a key technique in mathematical epidemiology that explores the sensitivity of the system to parameter variations, important trajectories like basic reproduction number (R_0). The normalized forward sensitivity index quantifies relative changes in outcomes due to changes in parameters. This analysis helps prioritize intervention strategies by highlighting the parameters that significantly impact disease transmission. A positive value of the index suggests that scaling up the param-

eter boosts disease spread, while a negative index reveals that increasing the parameter aids in controlling disease.

Parameters	Sensitivity index, R_O
β	+1.0000
η_1	+0.1964
η_2	+0.2455
η_3	+0.1498
η_4	+0.0783
Φ	-0.2541
Θ	-0.1906
Ω	0.0000
V	-0.2156
E	-0.1672
Γ	-0.1275
X	-0.0513
μ_H	-0.3408
z	-0.2957
τ	-0.2957

Figure 4.3: Table for Normalized Sensitivity Measures of Model Parameters

Sensitivity analysis reveals that the transmission rate (β) exerts the strongest positive effect on R_0 $(\beta = +1.0000)$, indicating that a proportional change in β leads to an equivalent proportional change in R_0. This highlights the importance of interventions, such as insecticide-treated nets and indoor residual spraying, in effectively reducing transmission. The infectivity parameters $(\eta_1, \eta_2, \eta_3$ and $\eta_4)$ also have positive indices, indicating that increased infectiousness from specific compartments particularly non-conflict infected humans and infectious mosquitoes will significantly increase R_0. Negative sensitivity indices identify parameters that help reduce transmission when increased. The human death rate (μ_H) and mosquito mortality parameters (Z) and (τ) are among the most influential, suggesting that measures that shorten the life span of mosquitoes or infected individuals substantially reduce R_0. Recovery and disease progression rates $(\Phi, \Theta, v, e, \epsilon, \gamma, x, \psi)$ also contribute negatively, with (Φ) and v being particularly important as they shorten the infectious period. Interestingly, the treatment initiation rate (ω) has no direct effect on R_0 in this formulation, indicating that its influence may operate indirectly through other model processes. In summary, the most effective strategies

for controlling malaria in this setting should focus on reducing β, increasing mosquito mortality rates (Z, τ), and accelerating recovery or removal from infectious states (Φ, υ), particularly in conflict-affected areas where treatment access is constrained.

4.1.12 Simulations Parameters of the Model

Model simulation is done by use of the Runge-Kutta method, and used to perform numerical simulations by the fourth-order Runge-Kutta method in MATLAB is employed to analyze the dynamic behavior of the model's state variables based on the given parameters. Numerical simulations is performed taking care of initial conditions and parameters provided above and results of are presented graphically as shown below.

4.1.12.1 Impact of malaria on all compartmental model

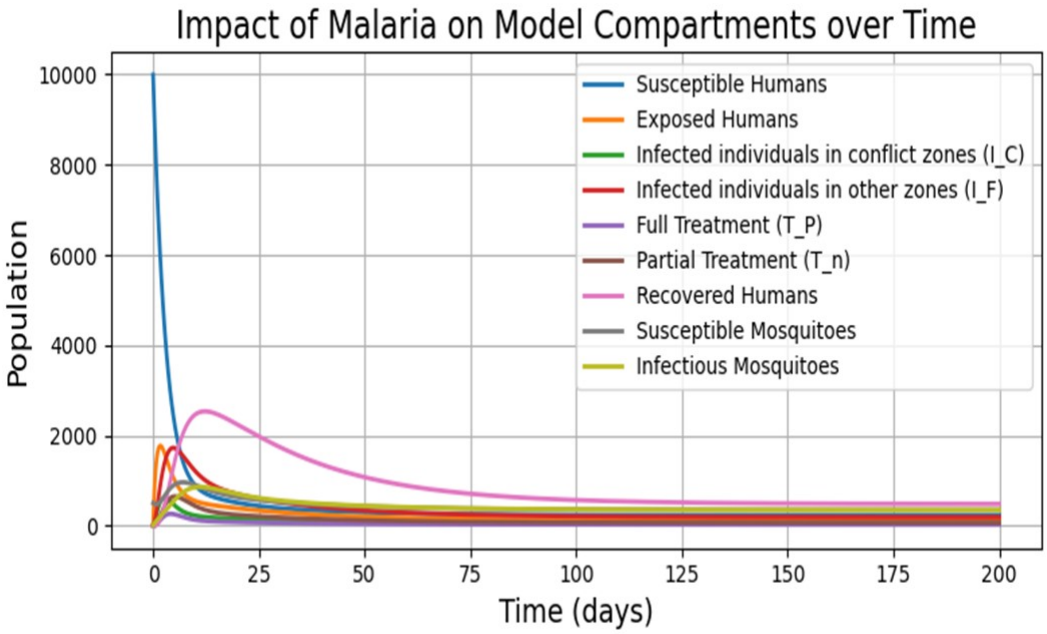

Figure 4.4: Total Human Population over Time in absence of Malaria

Figure 4.4 shows the temporal malaria transmission dynamics over a 200-day period across various model compartments. In the early stages, the class of humans who have not acquired infection reduces considerably as a consequence of rapid exposure of infection, while number of exposed and infected people increases significantly, reflecting disease's rapid spread. The populations of fully, partially, and recovered humans then grow as treatment and recovery procedures are implemented, with the recovered class

eventually taking the lead. In the meantime, populations of susceptible and infected mosquitoes stabilize at lower equilibrium levels, continuing transmission but with less vigor. The system as a whole converges toward an endemic equilibrium, where all compartments stabilize, underscoring the fact that malaria still exists in the population in spite of interventions.

4.1.12.2 Impact of Malaria on the Total Population without any Intervention

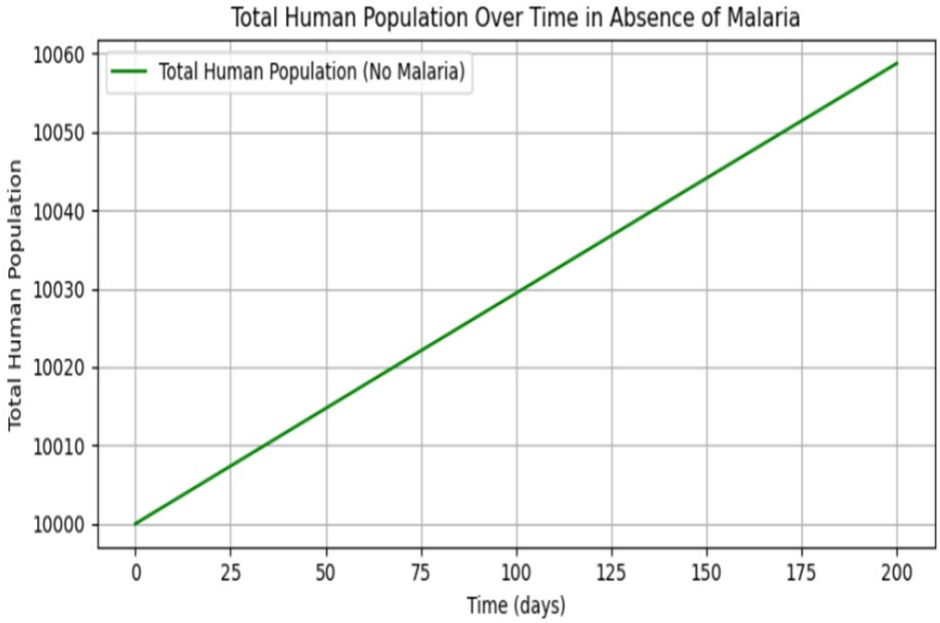

Figure 4.5: Total Human Population over Time in absence of Malaria

Figure 4.5 illustrates the behavior of the overall human population over time over time without the presence of malaria infection. With malaria transmission parameters set to zero, there is no disease-induced mortality or infection-related transitions, and population change is governed solely by natural birth and death rates. The curve shows a gradual and steady increase in total population due to the consistent recruitment rate (π=0.6849) exceeding the natural mortality rate. Since no individuals enter exposed or infectious compartments, the entire population remains in the susceptible and recovered states, with minimal losses due to natural death. This trend reflects the ideal scenario where, in the absence of malaria, the human population would grow predictably

without disruption, underscoring the significant demographic burden malaria imposes in endemic settings.

4.1.12.3 The Impact of Malaria on Treated Population over Time

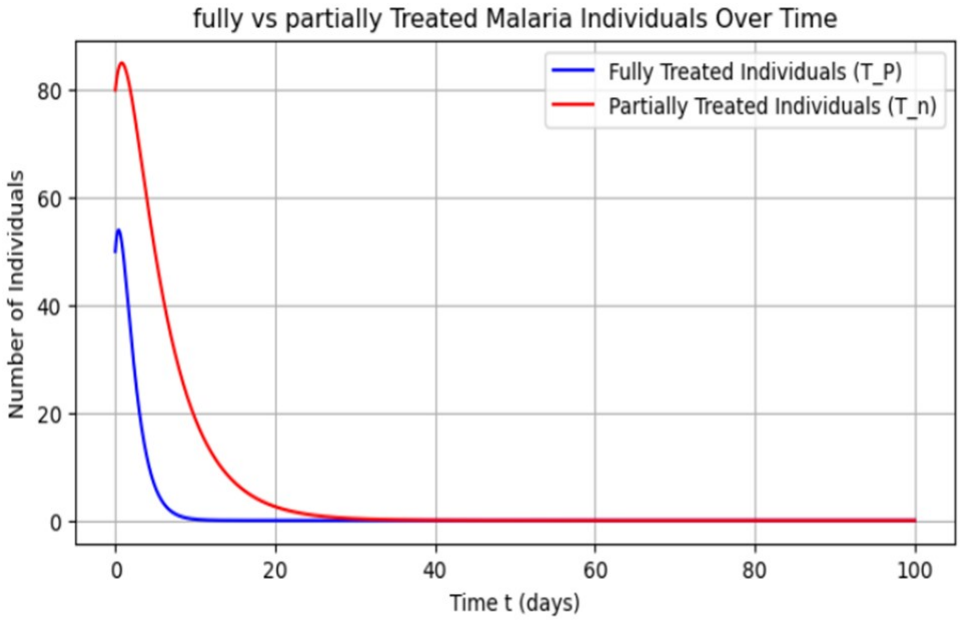

Figure 4.6: Total Human Population over Time in absence of Malaria

Figure 4.6 illustrates the progression of malaria-infected individuals undergoing full treatment (T_P) and partial treatment (T_n) over time. Initially, the number of partially treated individuals is higher, but both compartments exhibit a declining trend as treatment progresses. Fully treated individuals decline more rapidly, reflecting the higher recovery and transition rates associated with effective treatment. In contrast, the slower decline in the partially treated group suggests lower recovery efficacy or incomplete adherence, resulting in prolonged infection duration. Over time, both populations approach zero, indicating the eventual clearance of infections with sustained treatment efforts. This highlights the critical importance of full treatment coverage to effectively reduce the malaria burden.

4.1.12.4 The Impact of Malaria in Conflict Zones and other Zones

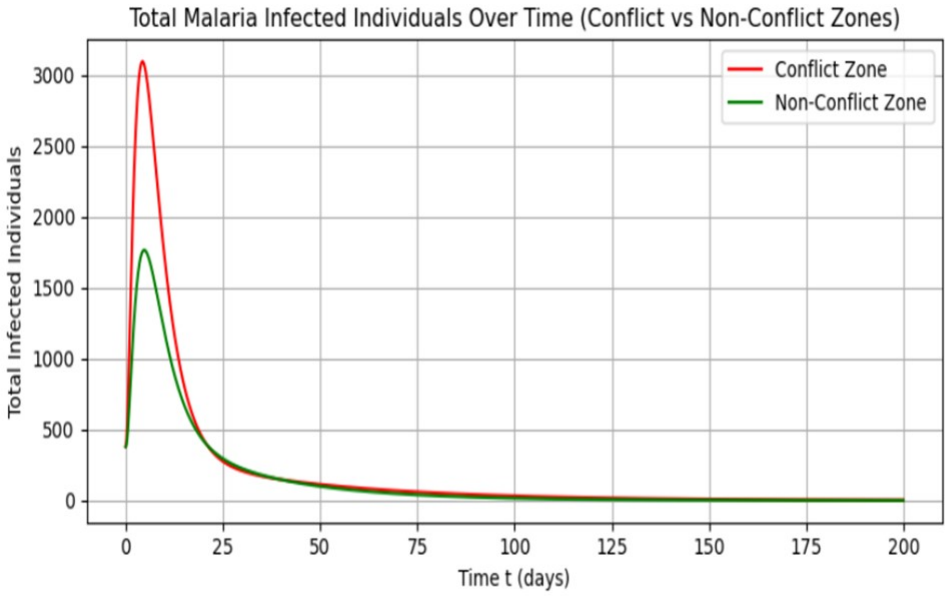

Figure 4.7: Total Malaria Infected Individuals Over time (Conflict vs Non-Conflict Zones)

Figure 4.7 compares the number of malaria-infected individuals over time between conflict as well as non-conflict zones. It clearly shows that the conflict zone experiences a significantly higher and more sustained burden of infection. This is due to the increased transmission rate and reduced treatment access modeled for conflict zones, resulting in a rapid rise and slower decline of infections. In contrast, the non-conflict zone shows a lower peak and quicker stabilization, reflecting better healthcare access and treatment efficacy. This trend highlights the critical impact of conflict on malaria dynamics, emphasizing the need for targeted intervention and healthcare support in vulnerable regions.

4.1.12.5 Comparison of Fully and Partially Treated Individuals over Time

Figure 4.8 illustrates the progression of malaria-infected individuals undergoing full treatment (T_P) and partial treatment (T_n) over time. Initially, the number of partially treated individuals is higher, but both compartments exhibit a declining trend as treatment progresses. Fully treated individuals decline more rapidly, reflecting the higher

recovery and transition rates associated with effective treatment. In contrast, the slower decline in the partially treated group suggests lower recovery efficacy or incomplete adherence, resulting in prolonged infection duration. Over time, both populations approach zero, indicating the eventual clearance of infections with sustained treatment efforts. This highlights the critical importance of full treatment coverage to effectively reduce the malaria burden.

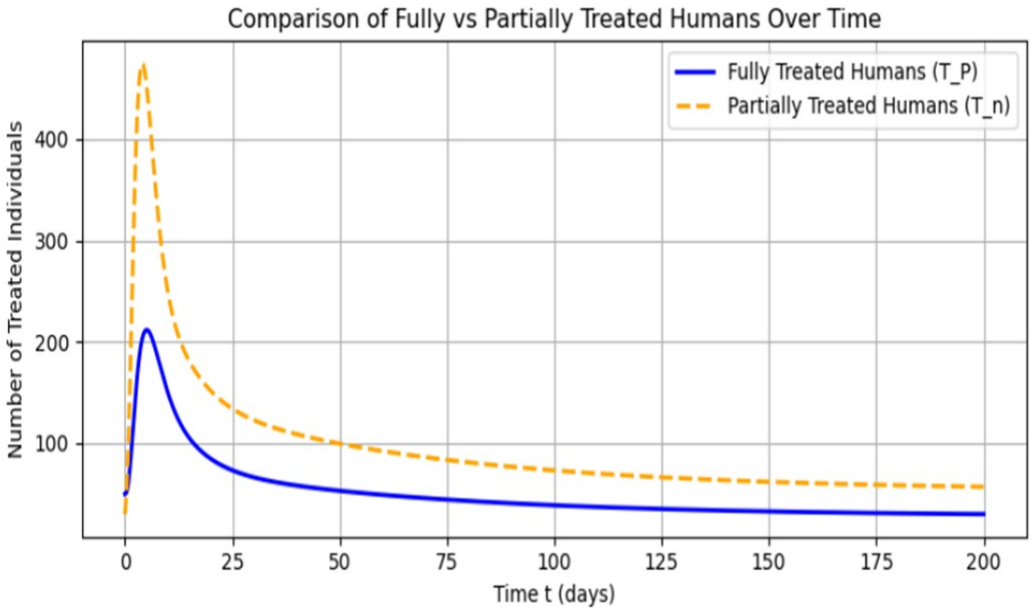

Figure 4.8: Full vs Partially treated Individuals Over Time

4.1.12.6 Susceptible Population with time at Varying Force of Infection

Figure 4.9 illustrates how varying levels, reflecting the force of disease transmission (β) influence the trajectory associated pertaining to the susceptible segment of the human population as time progresses in the context of susceptible individuals. As the force of infection increases (from β= 0.1 to β= 0.7), the decline in the susceptible population becomes more rapid and pronounced. This reveals that higher transmission potential leads to more individuals transitioning from among the compartment of susceptible at a faster rate due to infection. The lower values β the decrease in susceptible is slower and stabilizes at a higher population level, suggesting lower disease spread. Overall, the graph underscores the critical role of infection pressure in driving susceptibility dynam-

ics, demonstrating that intensified exposure to infectious vectors in high-transmission for instance conflict zones could severely deplete the susceptible pool within a short time frame.

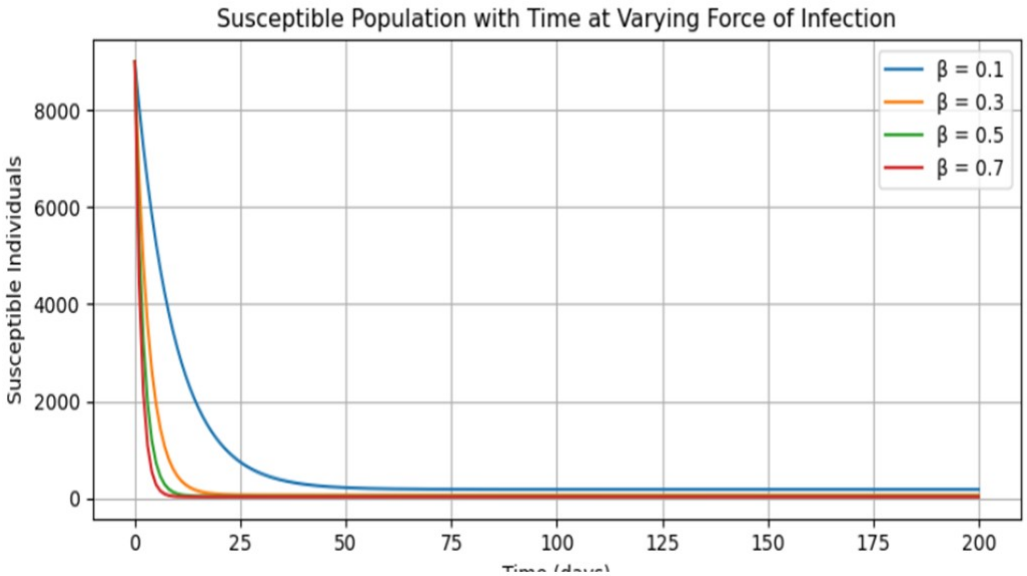

Figure 4.9: Susceptible Population with Time at Varying Force of Infection

4.1.12.7 Implication of Malaria on Total Human Population over Time

The figure 4.10 illustrates the consequences of malaria with respect to the overall human population as it changes over time, comparing two scenarios: one with ongoing malaria transmission and one without the disease. The red curve represents the total population under the influence of malaria, while the green dashed line shows the population trajectory in the absence of malaria-related infections and treatment dynamics. Initially, both populations may be similar, but as time progresses; the red curve tends to remain below the green one, reflecting the cumulative impact of malaria on population size. This includes deaths due to infection, reduced recovery, and prolonged treatment periods, which together suppress population growth. The gap between the two curves highlights the burden malaria places on public health and demographic stability, especially in regions with limited access to effective interventions.

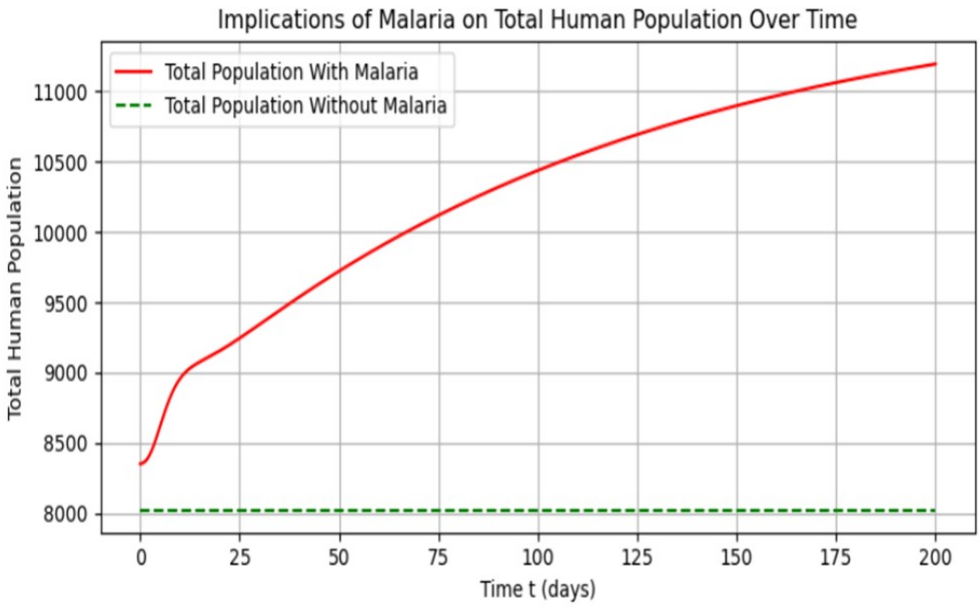

Figure 4.10: Malaria on Total Human Population over Time

4.1.12.8 Implication of Malaria Treatment on Total Population over Time

Figure 4.11 compares the total human population over time under two scenarios: with malaria treatment and without malaria treatment. In the untreated case (red dashed line), the total population declines more rapidly due to increased morbidity and mortality caused by uncontrolled malaria infections. Conversely, the treated case (green solid line) shows a more stable population size, with only a mild decline followed by gradual stabilization. This demonstrates that effective therapy not only mitigates the disease burden but also helps maintain a healthier and more stable population size. The divergence gap between the two curves widens over time, emphasizing the long-term benefits of implementing widespread malaria treatment programs.

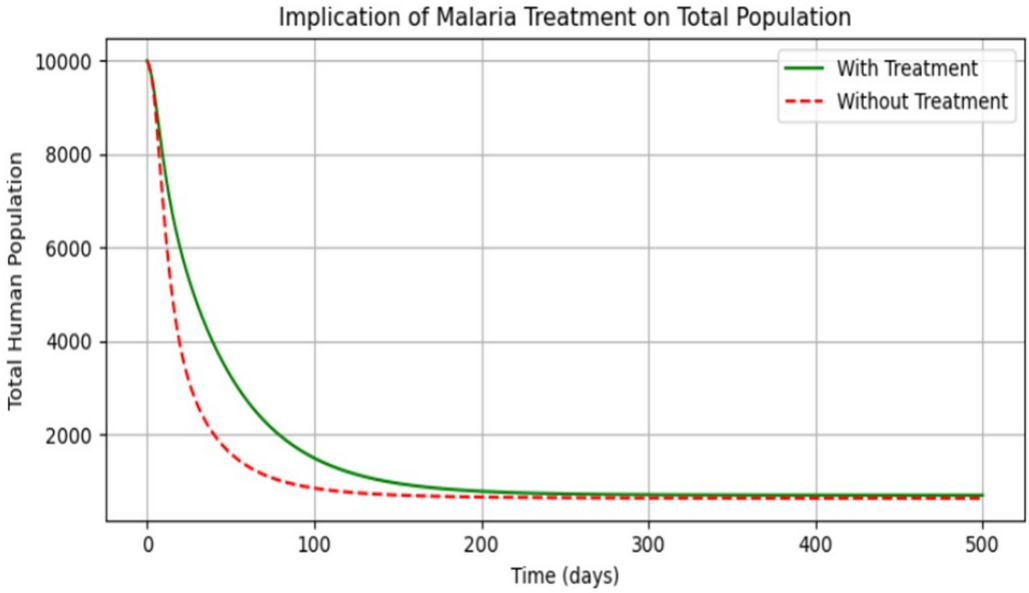

Figure 4.11: Malaria Treatment on Total Population over Time

4.1.12.9 Effects of Malaria Recovery rate on total population over Time

Figure 4.12 illustrates the implications of varying recovery rates (γ) on the total human population over time in a malaria-endemic setting. As shown, scenarios with higher recovery rates ($\gamma = 0.2$) maintain a more stable and higher total population, while lower recovery rates ($\gamma = 0.05$) lead to more significant population decline or stagnation. This behavior arises from the fact that a lower rate at which individuals recover slows down as transition for individuals moving from the infected compartment to the recovered compartment, increasing the period of infection, and in turn raising the disease burden and malaria-induced mortality. Conversely, higher recovery rates help reduce the infectious population more rapidly, mitigating disease spread and associated deaths, thereby preserving the total population size. The graph underscores the critical role of improving recovery for instance through effective treatment in sustaining population health and controlling malaria impact.

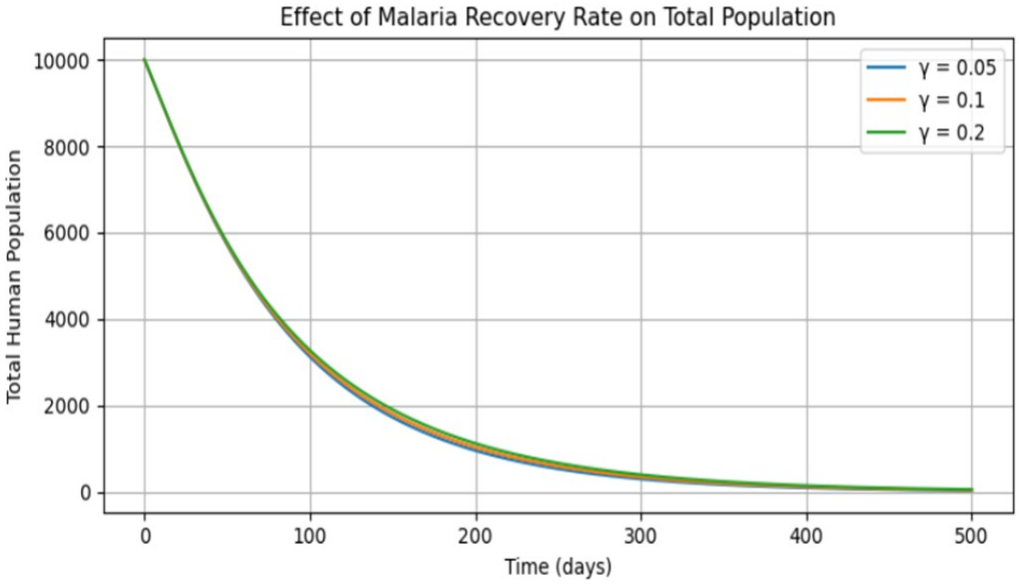

Figure 4.12: Malaria Treatment on Total Population over Time

4.1.12.10 Relationship Between Infected Individuals In Conflict Zones and Non-Conflict Zones

Figure 4.13 demonstrates the relationship between malaria infection levels within conflict-affected and non-affected regions indicates that infections are consistently higher in conflict areas throughout the simulation. The non-linear curve reveals that infections in conflict zones escalate more quickly and reach higher peaks compared to non-conflict zones. This is attributed to factors like weakened healthcare, displacement, and limited access to treatment. Minor fluctuations in the data may indicate the instability of these regions. The graph underscores the greater malaria burden in conflict zones and the critical requirement for targeted interventions and resource distribution in these areas.

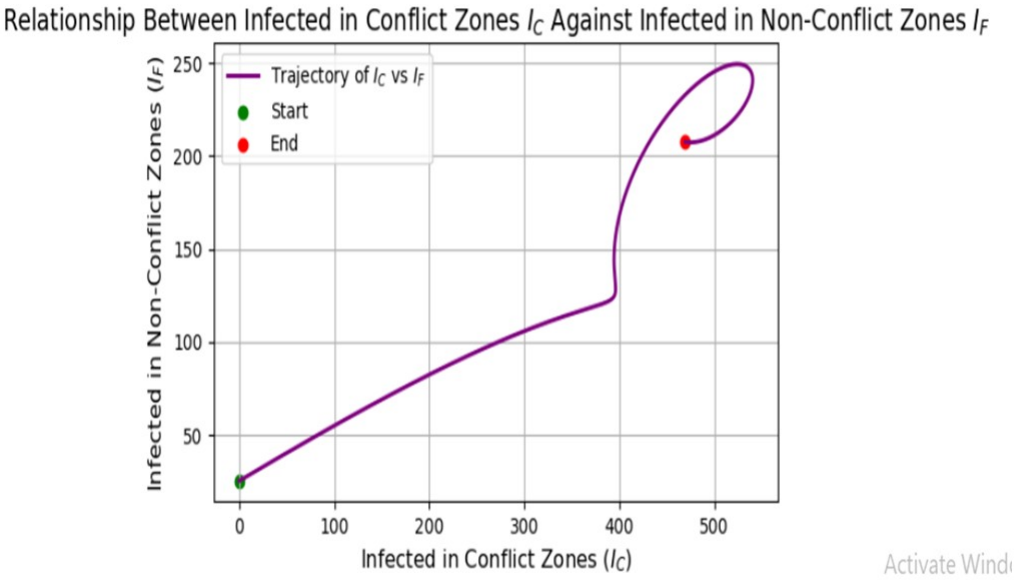

Figure 4.13: Infection Comparison Between Populations in Conflict Zones and Infected Individuals in Non-Conflict Areas

4.1.12.11 Relationship Between Fully and Partially Treated Individuals

Figure 4.14 shows relationship Between T_P and T_n showing the interaction between fully treated individuals T_P and partially treated individuals T_n in malaria treatment over time. There is a nonlinear, positively correlated relationship observed, where initially an increase in partially treated individuals leads to an increase in fully treated individuals, suggesting a shared treatment framework. However, after a certain point, the growth rate of fully treated individuals slows down even as partially treated individuals continue to rise. This may indicate saturation in treatment capacity or challenges in prioritization due to limited resources. Oscillations in the curves could represent inconsistencies in treatment, drug shortages, or periodic interventions like mass treatment campaigns. The graph highlights that although both treatment types increase, maintaining proportional growth in full treatment coverage is a challenge, stressing the need for stronger treatment programs in malaria-endemic or resource-limited areas.

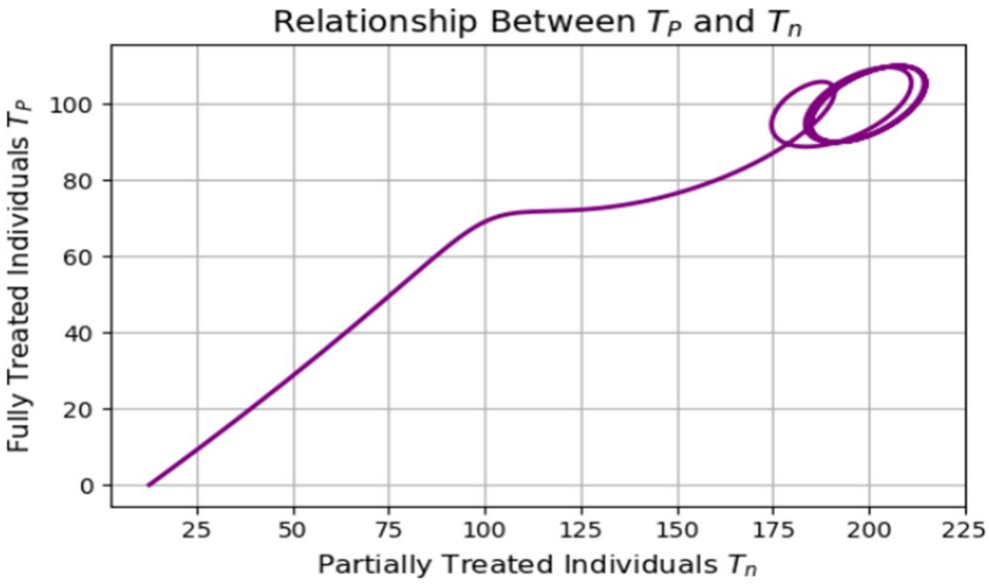

Figure 4.14: Fully and Partially Treated Individuals

4.1.12.12 Relationship Between Total Treated and Total Infected Individuals

Figure 4.15 illustrates an increasing, though nonlinear, relationship between total treated individuals and total infected individuals. Initially an upward trend in infections contributes to a steady increase in treated individuals, indicating a responsive healthcare system. However, as infections escalate, particularly in conflict zones, the growth of treated individuals' levels off, suggesting a saturation or delay in treatment coverage. This could be attributed to healthcare infrastructure limitations and access challenges. Furthermore, the fact that partial treatment exceeds full treatment indicates a significant treatment gap, emphasizing the necessity for enhanced healthcare infrastructure and targeted interventions in conflict-affected areas.

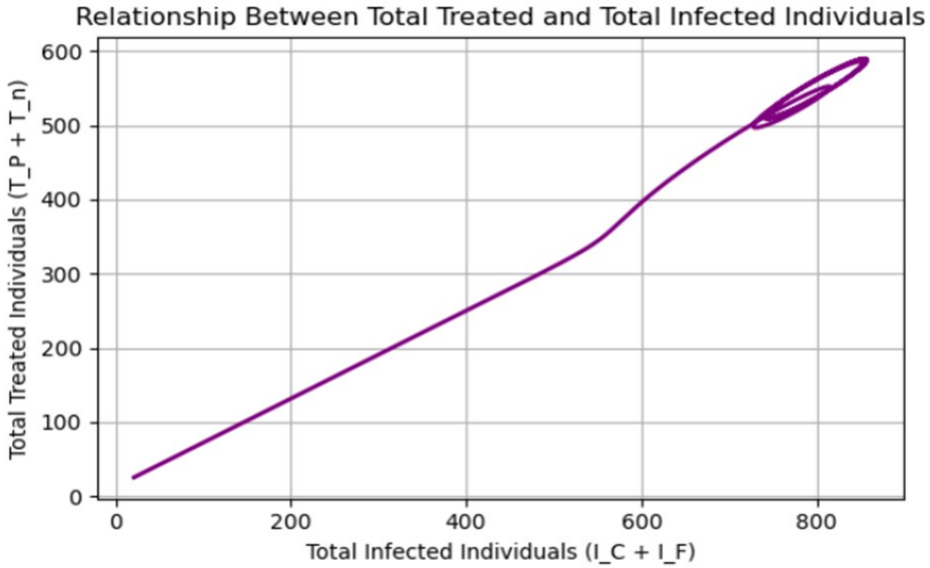

Figure 4.15: Total Treated and Total Infected Individuals

CHAPTER FIVE

SUMMARY, CONCLUSION AND RECOMMENDATION

5.1 Summary and Conclusion

The study developed and analyzed a deterministic mathematical framework on malaria transmission and treatment a case of conflict zones. The framework divided the population of humans into seven compartments: susceptible-exposed, individuals infected in conflict zones- infected individuals in non-conflict zones-fully treated individual,-partially treated individuals- and recovered individuals, along with two compartments for mosquitoes: susceptible and infected mosquitoes, totaling nine compartments. The mathematical framework governing first-order differential equations were developed and valid solutions were computed, ensuring all state variables remained non-negative and bounded. The basic reproduction number was computed through the next Generation Matrix Method to confirm the analysis of local stability at the disease-free equilibrium. Sensitivity evaluation suggested that transmission rates, and treatment coverage are crucial for malaria persistence, highlighting the importance of timely diagnosis and targeted interventions in conflict-affected areas. Based on the study the following conclusions were made; High malaria burden in conflict zones emphasizes the negative impact of conflict on disease control, pointing to the vital need for specific healthcare interventions and better access to treatment in these risky regions as shown by graph of the impact related to malaria dynamics in conflict-impacted zones and other zones. The study also concluded that full malaria treatment is more effective in promoting recovery and shortening infection duration compared to partial treatment. It points out that incomplete treatment can lead to longer infections and ongoing transmission. Consequently, adhering to full treatment is crucial for long-term malaria control and disease elimination as shown by graph of comparison of fully and partially treated individuals over time. Sensitivity analysis was used to examine the assessment of the equilibrium stability of the disease-free and endemic equilibrium points. Findings indicate, when basic reproduction number $R_0 < 1$, the disease-free equilibrium is locally and globally stable, suggesting that reducing R_0 below one can limit disease spread. Conversely, the endemic equilibrium is asymptotically stable when $R_0 > 1$. Numerical analysis revealed that malaria spreads more rapidly in the conflict zones than other zones, but proper treatment can effectively eradicate the disease.

5.2 Recommendation

The study leads to the following recommendation:

i. Adopt hybrid and spatially explicit models that capture displacement and localized transmission dynamics.

ii. Researchers should utilize multiple data sources to improve model accuracy.

iii. Bayesian and particle based calibration methods are recommended to manage parameter uncertainty and generate credible probabilistic forecast sunder data limitations.

REFERENCES

Agusto, F. B., Del Valle, S. Y., Blayneh, K. W., Ngonghala, C. N., Goncalves, M. J., Li, N., Zhao, R., and Gong, H. (2013). The impact of bed-net use on malaria prevalence. *Journal of theoretical biology*, 320:58–65.

Amadi, M., Shcherbacheva, A., and Haario, H. (2021). Agent-based modelling of complex factors impacting malaria prevalence. *Malaria journal*, 20:1–15.

Anderson, R. (1991). *Infectious diseases of humans: dynamics and control*. Oxford University Press.

Aron, J. L. (1988). Mathematical modelling of immunity to malaria. *Mathematical Biosciences*, 90(1-2):385–396.

Arora, N., C Anbalagan, L., and Pannu, A. K. (2021). Towards eradication of malaria: is the who's rts, s/as01 vaccination effective enough? *Risk Management and Healthcare Policy*, pages 1033–1039.

Ashley, E. A., Dhorda, M., Fairhurst, R. M., Amaratunga, C., Lim, P., Suon, S., Sreng, S., Anderson, J. M., Mao, S., Sam, B., et al. (2014). Spread of artemisinin resistance in plasmodium falciparum malaria. *New England Journal of Medicine*, 371(5):411–423.

Autino, B., Corbett, Y., Castelli, F., and Taramelli, D. (2012). Pathogenesis of malaria in tissues and blood. *Mediterranean journal of hematology and infectious diseases*, 4(1).

Bakary, T., Boureima, S., and Sado, T. (2018). A mathematical model of malaria transmission in a periodic environment. *Journal of biological dynamics*, 12(1):400–432.

Bhatt, S., Weiss, D., Cameron, E., Bisanzio, D., Mappin, B., Dalrymple, U., Battle, K., Moyes, C., Henry, A., Eckhoff, P., et al. (2015). The effect of malaria control on plasmodium falciparum in africa between 2000 and 2015. *Nature*, 526(7572):207–211.

Brock, A. R., Ross, J. V., Parikh, S., and Esterman, A. (2018). The role of antimalarial quality in the emergence and transmission of resistance. *Medical Hypotheses*, 111:49–54.

Chitnis, N., Hyman, J. M., and Cushing, J. M. (2008). Determining important parameters in the spread of malaria through the sensitivity analysis of a mathematical model. *Bulletin of mathematical biology*, 70:1272–1296.

Chiyaka, C., Mukandavire, Z., Das, P., Nyabadza, F., Hove-Musekwa, S. D., and Mwambi, H. (2010). Theoretical analysis of mixed plasmodium malariae and plasmodium falciparum infections with partial cross-immunity. *Journal of theoretical biology*, 263(2):169–178.

Collins, O. and Duffy, K. (2022). A mathematical model for the dynamics and control of malaria in nigeria. *Infectious disease modelling*, 7(4):728–741.

Conway, D. J. (2007). Molecular epidemiology of malaria. *Clinical Microbiology Reviews*, 20(1):188–204.

Diekmann, O., Heesterbeek, J. A. P., and Metz, J. A. J. (1990). On the definition and the computation of the basic reproduction ratio r 0 in models for infectious diseases in heterogeneous populations. *Journal of mathematical biology*, 28:365–382.

Dondorp, A. M., Fanello, C. I., Hendriksen, I. C., Gomes, E., Seni, A., Chhaganlal, K. D., Bojang, K., Olaosebikan, R., Anunobi, N., Maitland, K., et al. (2010). Artesunate versus quinine in the treatment of severe falciparum malaria in african children (aquamat): an open-label, randomised trial. *The Lancet*, 376(9753):1647–1657.

Eckhoff, P. A. (2011). A malaria transmission-directed model of mosquito life cycle and ecology. *Malaria journal*, 10:1–17.

Fatmaningsih, L., Aulia, M., Sa'id, I. B., et al. (2024). Genetic engineering of mosquitoes causes malaria. *Journal of Biomedical and Techno Nanomaterials*, 1(2):70–82.

Greenwood, B. (1997). The epidemiology of malaria. *Annals of Tropical Medicine & Parasitology*, 91(7):763–769.

Heffernan, J. M., Smith, R. J., and Wahl, L. M. (2005). Perspectives on the basic reproductive ratio. *Journal of the Royal Society Interface*, 2(4):281–293.

Hethcote, H. W. (2000). The mathematics of infectious diseases. *SIAM review*, 42(4):599–653.

Hoshen, M., Stein, W., and Ginsburg, H. (2001). Pharmacokinetic-pharmacodynamic modelling of the anti-malarial activity of mefloquine. *Parasitology*, 123(4):337–346.

Huang, F., Zhou, S., Zhang, S., Wang, H., and Tang, L. (2011). Temporal correlation analysis between malaria and meteorological factors in motuo county, tibet. *Malaria Journal*, 10(1):54.

Keeling, M. J. and Rohani, P. (2008). *Modeling infectious diseases in humans and animals*. Princeton university press.

Kermack, W. O. and McKendrick, A. G. (1927). A contribution to the mathematical theory of epidemics. *Proceedings of the royal society of london. Series A, Containing papers of a mathematical and physical character*, 115(772):700–721.

Khalil, H. K. and Grizzle, J. W. (2002). *Nonlinear systems*, volume 3. Prentice hall Upper Saddle River, NJ.

Kiszewski, A., Mellinger, A., Spielman, A., Malaney, P., Sachs, S. E., Sachs, J., et al. (2004). A global index representing the stability of malaria transmission. *American Journal of tropical medicine and hygiene*, 70(5):486–498.

Koella, J. and Antia, R. (2003). Epidemiological models for the spread of anti-malarial resistance. *Malaria Journal*, 2:1–11.

Macdonald. G, M. G. (1957). The epidemiology and control of malaria.

Mbogo, R. W., Luboobi, L. S., and Odhiambo, J. W. (2018). A stochastic model for malaria transmission dynamics. *Journal of applied mathematics*, 2018(1):2439520.

Menéndez, C., Bardají, A., Sigauque, B., Sanz, S., Aponte, J. J., Mabunda, S., and Alonso, P. L. (2010). Malaria prevention with iptp during pregnancy reduces neonatal mortality. *PloS one*, 5(2):e9438.

Miller, L. H., Baruch, D. I., Marsh, K., and Doumbo, O. K. (2002). The pathogenic basis of malaria. *Nature*, 415(6872):673–679.

Mkubwa, B., Kagura, J., Chirwa, T., Ibisomi, L., and Kinyanjui, S. (2022). Determinants of utilization of malaria preventive measures during pregnancy among women aged 15 to 49 years in kenya: an analysis of the malaria indicator survey 2020. *Malaria Journal*, 21(1):398.

Mukhtar, A. Y., Munyakazi, J. B., Ouifki, R., and Clark, A. E. (2018). Modelling the effect of bednet coverage on malaria transmission in south sudan. *PLoS One*, 13(6):e0198280.

Mwangangi, J. M., Mbogo, C. M., Orindi, B. O., Muturi, E. J., Midega, J. T., Nzovu, J., Gatakaa, H., Githure, J., Borgemeister, C., Keating, J., et al. (2013). Shifts in malaria vector species composition and transmission dynamics along the kenyan coast over the past 20 years. *Malaria journal*, 12(1):13.

Ngwa, G. A. and Shu, W. S. (2000). A mathematical model for endemic malaria with variable human and mosquito populations. *Mathematical and computer modelling*, 32(7-8):747–763.

Organization, W. H. (2022). *Guidelines for drinking-water quality: incorporating the first and second addenda*. World Health Organization.

Otieno, G., Koske, J. K., and Mutiso, J. M. (2016). Cost effectiveness analysis of optimal malaria control strategies in kenya. *Mathematics*, 4(1):14.

Paaijmans, K. P., Read, A. F., and Thomas, M. B. (2009). Understanding the link between malaria risk and climate. *Proceedings of the National Academy of Sciences*, 106(33):13844–13849.

Rajnarayanan, A. and Kumar, M. (2024). Analysis of a mathematical model for malaria using data-driven approach. *arXiv preprint arXiv:2409.00795*.

Ross, R. (1911). *The prevention of malaria*. John Murray.

Smith, D. L., McKenzie, F. E., Snow, R. W., and Hay, S. I. (2007). Revisiting the basic reproductive number for malaria and its implications for malaria control. *PLoS biology*, 5(3):e42.

Smith, T., Killeen, G. F., Maire, N., Ross, A., Molineaux, L., Tediosi, F., Hutton, G., Utzinger, J., Dietz, K., Tanner, M., et al. (2006). Mathematical modeling of the impact of malaria vaccines on the clinical epidemiology and natural history of plasmodium falciparum malaria: Overview. *American Journal of Tropical Medicine and Hygiene*, 75(2):1.

Tatem, A. J., Gething, P. W., Smith, D. L., and Hay, S. I. (2013). Urbanization and the global malaria recession. *Malaria journal*, 12:1–11.

Tchuenche, J. M., Chiyaka, C., Chan, D., Matthews, A., and Mayer, G. (2011). A mathematical model for antimalarial drug resistance. *Mathematical medicine and biology: a journal of the IMA*, 28(4):335–355.

Van den Driessche, P. and Watmough, J. (2002). Reproduction numbers and subthreshold endemic equilibria for compartmental models of disease transmission. *Mathematical biosciences*, 180(1-2):29–48.

Wongsrichanalai, C., Barcus, M. J., Muth, S., Sutamihardja, A., and Wernsdorfer, W. H. (2007). A review of malaria diagnostic tools: microscopy and rapid diagnostic test (rdt). *Defining and Defeating the Intolerable Burden of Malaria III: Progress and Perspectives: Supplement to Volume 77 (6) of American Journal of Tropical Medicine and Hygiene*.

APPENDIX I: Python Code for Simulating Profiles

import numpy as np

import matplotlib.pyplot as plt

Time vector (days)

t = np.linspace(0, 250, 600)

$I_C > I_F and T_n > T_P$ for all t, consistent with your assumptions.

$I_C 0, k_I C = 80.0, 0.050$

$I_F 0, k_I F = 50.0, 0.040$

$T_P 0, k_T P = 30.0, 0.060$

$T_n 0, k_T N = 60.0, 0.045$

$I_V 0, k_I V = 40.0, 0.060$

$I_C = I_C 0 * np.exp(-k_I C * t)$

$I_F = I_F 0 * np.exp(-k_I F * t)$

$T_P = T_P 0 * np.exp(-k_T P * t)$

$T_n = T_n 0 * np.exp(-k_T N * t)$

$I_V = I_V 0 * np.exp(-k_I V * t)$

Total infected burden (humans under infection/treatment + infectious vectors) Total =

$I_C + I_F + T_P + T_n + I_V$

— Plot —

plt.figure(figsize=(8, 4))

plt.plot(t, Total, linewidth=3,

label='Total infected burden ($I_C + I_F + T_P + T_n + I_V$)', $color =' black')$

$plt.plot(t, I_C, label =' Infected(conflict)I'_C$, linestyle='-')

plt.plot(t, $I_F, label =' Infected(non - conflict)$$I_F$', linestyle='-')

plt.plot(t, $T_P, label =' Fullytreated$$I_P$', linestyle='–')

plt.plot(t, $T_n, label =' Partiallytreated$$I_N$', linestyle='–')

plt.plot(t, $I_V, label =' Infectiousmosquitoes$$I_V$', linestyle=':')

plt.title('Malaria Infected Burden Over Time at DFE ($R_0 < 1$)')

plt.xlabel('Time (days)')

plt.ylabel('Number of individuals (or vectors)')

plt.grid(True, alpha=0.5)

plt.legend()

plt.tight$_{l}ayout()$

$plt.show()$

import numpy as np

import matplotlib.pyplot as plt

from scipy.integrate import odeint

— 1. Define parameters —

params = π: 0.00006849,

ζ: 0.4,

α: 0.3,

μ: 0.000039,

ρ: 0.05,

: 0.5,

ϕ: 0.3,

Θ: 0.15,

ω: 0.2,

ν: 0.3,

ϵ: 0.08,

γ: 0.2,

: 0.3,

: 0.1,

Λ: 80,

ψ: 0.3,

τ: 0.1

— 2. Initial conditions —

[S$_H, E, I_C, I_F, T_P, T_n, R, S_V, I_V$]

$initial_conditions = [9990, 5, 2, 1, 0, 0, 2, 1000, 0]$

APPENDIX II:ISERC Approval

THARAKA UNIVERSITY

P.O BOX 193-60215,
MARIMANTI, KENYA

Website: https://tharaka.ac.ke
Social Media: tharakauni
Email: info@tharaka.ac.ke
Phone : +254 745 838 353

INSTITUTIONAL SCIENTIFIC AND ETHICS REVIEW COMMITTEE

10th April, 2025

REF: TUNISERC/NSEC/ M047

Dear Nguu Alex Ngatia,

RE: Mathematical Modelling of Malaria Transmission and Treatment: A Case of Conflict Zones

This is to inform you that ***Tharaka University ISERC*** has reviewed and approved your above research proposal. Your application approval number is ***ISERC04023.*** The approval period is ***10th April, 2025 – 10th April, 2026.***

This approval is subject to compliance with the following requirements;

i. Only approved documents including (informed consents, study instruments, MTA) will be used
ii. All changes including (amendments, deviations, and violations) are submitted for review and approval by ***Tharaka University ISERC.***
iii. Death and life-threatening problems and serious adverse events or unexpected adverse events whether related or unrelated to the study must be reported to ***Tharaka University ISERC*** within 72 hours of notification
iv. Any changes, anticipated or otherwise that may increase the risks or affected safety or welfare of study participants and others or affect the integrity of the research must be reported to ***Tharaka University ISERC*** within 72 hours
v. Clearance for export of biological specimens must be obtained from relevant institutions.
vi. Submission of a request for renewal of approval at least 60 days prior to expiry of the approval period. Attach a comprehensive progress report to support the renewal.
vii. Submission of an executive summary report within 90 days upon completion of the study to ***Tharaka University ISERC.***

Prior to commencing your study, you will be expected to obtain a research license from National Commission for Science, Technology and Innovation (NACOSTI) https://research-portal.nacosti.go.ke and also obtain other clearances needed.

Yours sincerely,

Dr. Fidelis Ngugi
Chairperson, ISERC Tharaka University

TUN is ISO 9001:2015 Certified... *Education for Freedom/Elimu ni Uhuru*

APPENDIX III:Research Authorization (NACOSTI)

REPUBLIC OF KENYA

NATIONAL COMMISSION FOR SCIENCE,TECHNOLOGY & INNOVATION

Ref No: **874654**

Date of Issue: **30/July/2025**

RESEARCH LICENSE

This is to Certify that Mr.. ALEX NG'ATIA NG'ATIA of Tharaka University, has been licensed to conduct research as per the provision of the Science, Technology and Innovation Act, 2013 (Rev.2014) in Tharaka-Nithi on the topic: MATHEMATICAL MODELINGOF MALARIA AND TREATMENT : A CASE OF CONFLICT ZONES for the period ending : 30/July/2026.

License No: **NACOSTI/P/25/4176880**

874654

Applicant Identification Number

Ag. Director General
NATIONAL COMMISSION FOR SCIENCE,TECHNOLOGY & INNOVATION

Verification QR Code

NOTE: This is a computer generated License. To verify the authenticity of this document, Scan the QR Code using QR scanner application.

See overleaf for conditions